MINIMIZING SECULAR J_2 PERTURBATION EFFECTS ON SATELLITE FORMATIONS

THESIS

Jonathan W. Wright, Second Lieutenant, USAF

AFIT/GA/ENY/08-M08

DEPARTMENT OF THE AIR FORCE
AIR UNIVERSITY

AIR FORCE INSTITUTE OF TECHNOLOGY

Wright-Patterson Air Force Base, Ohio

AFIT/GA/ENY/08-M08

MINIMIZING SECULAR J_2 PERTURBATION EFFECTS ON SATELLITE FORMATIONS

THESIS

Presented to the Faculty

Department of Aeronautics and Astronautics

Graduate School of Engineering and Management

Air Force Institute of Technology

Air University

Air Education and Training Command

in Partial Fulfillment of the Requirements for the

Degree of Master of Science in Astronautical Engineering

Jonathan W. Wright, BAE
Second Lieutenant, USAF

March 2008

AFIT/GA/ENY/08-M08

MINIMIZING SECULAR J_2 PERTURBATION EFFECTS ON SATELLITE FORMATIONS

Jonathan W. Wright, BAE
Second Lieutenant, USAF

Approved:

Nathan A. Titus (Chairman)	14 Mar 08 date
Kerry D. Hicks (Member)	14 Mar 08 date
William E. Wiesel (Member)	14 Mar 08 date

AFIT/GA/ENY/08-M08

Abstract

The purpose of this thesis is to examine the secular effects of the J_2 oblateness perturbation on close proximity satellites. The main objective is to analyze the deputy's position and velocity with respect to the chief and adjust the initial conditions of the deputy in an attempt to minimize the secular effects of J_2 perturbations. Previous work has provided a method of obtaining a closed form solution for J_2 invariance with co-planar orbits. Therefore, this work will primarily consider deputy orbits that experience motion outside of the chief's orbital plane.

Upon determining the required initial conditions, the invariance will be verified through numerical integration. The method will be considered successful when it is able to reduce secular effects to near numerical tolerances.

To my Supportive Family

Acknowledgements

I would like to thank my faculty advisor Lt Col Titus for his continued support and guidance throughout the entire process of completing my thesis. I would also like to thank all of the members of my committee for their continued efforts as professors and their individual contribution to my education. In addition, I would like to thank my undergraduate Orbital Mechanics professor for creating an interest in astronautics that helped lead to my pursuit of a master's degree in this field.

Jonathan W. Wright

Table of Contents

List of Figures

List of Symbols

a	= Orbit semi-major axis
e	= Orbit eccentricity
i	= Orbit inclination
Ω	= Orbit longitude of the ascending node
ω	= Orbit argument of perigee
ν	= Orbit true anomaly
i_d	= "d" Subscript indicates the element is for the deputy satellite
δ	= Difference in the deputy's and chief's orbital element
M	= Orbit mean anomaly
θ	= Chief's Argument of latitude
J_2	= Gravitational expansion coefficient of the second zonal harmonic
a_e	= Relative orbit major axis
x_d	= Coordinate of center of relative ellipse in the radial direction
y_d	= Coordinate of center of relative ellipse in the orbital direction
z_{max}	= Maximum out-of-plane displacement of the deputy
β	= Deputy's angular position on relative orbit
γ	= Deputy's relative ascending node
γ_z	= Angle of the deputy's out-of-plane oscillation
C_{oe}	= Chief's classical orbital elements
e_r	= Error value
ISS	= International Space Station
μ	= Gravitational Constant multiplied with Earth's mass

MINIMIZING SECULAR J_2 PERTURBATION EFFECTS ON SATELLITE FORMATIONS

I. Introduction

Objective

The concept of satellite formations opens the possibility for multiple applications. One important example is distributed aperture surveillance. Multiple sensors at different locations may observe an object, and the multiple vantage points allow the images to be refined. The result is a finer resolution than the sensors could provide individually. Another advantage of a cluster of small satellites would be the distribution of both capabilities and redundant systems. This would increase survivability and reliability by distributing redundant, mission critical systems amongst several smaller, individual satellites.

There could also be more flexibility when forced to reassign assets. If the formation has mission capable redundancies distributed amongst several smaller satellites, operators would have the option of reassigning redundant systems while keeping the primary assets on the current task. If the formation had a distribution of capabilities amongst several satellites, this could also allow flexibility in the case of rapid reassignment. In this situation would be possible to deploy mission critical assets quickly. This would allow these assets to accomplish more time sensitive tasks. Meanwhile, if the other assets in the cluster are less time sensitive a smaller, more fuel efficient maneuver can be made. This would allow for the completion of mission objectives without consuming more fuel than necessary.

While there are many benefits of satellite formations, there are some disadvantages, as well. One disadvantage is the amount of fuel required to maintain the formation. In the presence of perturbation accelerations, formations require significant fuel consumption in order to maintain the desired relative trajectories. For a Low Earth Orbit (LEO), the primary perturbations are due to the atmospheric drag, solar pressure, and the earth's oblateness. While drag forces are an important factor for individual satellite dynamics, the satellites would be affected similarly if the satellites were identical and maintained the same orientation. Therefore, the relative position and velocity will not be greatly affected. The perturbation acceleration due to the oblateness of the earth, commonly referred to as the J_2 perturbation, has the greatest effect on the relative motion and, effectively, the rate of fuel consumption.

It has been proposed that by adjusting the initial conditions of the formation, the perturbing accelerations may be reduced. Because the primary perturbation acceleration for LEO orbits is the J_2 oblateness perturbation, the objective of this thesis is to determine a method of adjusting the initial conditions to minimize the secular effects of the J_2 perturbation.

Approach

This thesis will attempt to minimize the secular effects of the J_2 perturbation accelerations while keeping in mind the desired relative geometry. The problem will be presented in the form of a fixed chief orbit and desired Relative Orbital Elements, and the solution will include a process of making changes to the desired set of Relative Orbital Elements in order to achieve near J_2 invariance.

In order to accomplish the objectives stated above, the approach taken in this research was to first describe the secular effects of the J_2 perturbation on the formation

parameters as a function of the relative geometry and the chief's Classical Orbital Elements (COE). The parameters used to describe the relative geometry were Relative Orbital Elements (ROE), an intuitive set of parameters that describe the size, shape, and orientation of the motion relative to the chief, in a manner analogous to how the COE describe the orbital motion about the earth.

Once the secular effects were defined in terms of the ROE, a nonlinear approach was developed to compute adjustments in the ROE, which reduced the effects of the secular drift.

II. Literature Review

Although the approach investigated in this work provides new insights into the effects of J_2 perturbations described by ROE, it is by no means the first attempt to understand and minimize the effect. In previous literature, the method is often referred to as establishing a "J_2 Invariant Formation", a term first coined by Schaub and Alfriend (6:78). Many others including Wiesel, Breger and How, and Sabitini and Tragesser have also added to the literature on this problem.

J_2 Invariance Method

One method to solve for J_2 invariant orbital elements has been established by Hanspeter Schaub and Kyle T. Alfriend (6:77-85). The method determined was based on momentum equations found from the first-order expansion of the Hamiltonian with respect to J_2. The system produced two equations that are functions of the chief's momentum elements. These were then converted back into classical orbital elements, resulting in expressions that were functions of the chief's classical orbital elements and three orbital element differences: δa, δi, and δe. This allows for one of the desired values to be fixed and a closed form solution obtained for the other two.

Though a solution is produced, the method does not allow for a significant amount of physical interpretation due to the solution set existing in momentum space. In addition, though this solution was based on a non-circular chief, the solution allows for a secular drift in the differences in the argument of perigee. In the event that the arguments of perigee become out of phase for a moderately eccentric chief and deputy, it becomes clear that the relative positions could vary greatly from the desired conditions. Also, the solution includes the tangent of the chief's inclination. Therefore, a singularity arises for

nearly polar orbits. Although a perfectly polar orbit cannot be obtained, a solution still exists; however, this solution requires considerably large contributions from to the other components.

Partial J_2 Invariance

Another method that approached partial J_2 invariance was presented by Breger and How (1:1-9). The method refers to "Partial Invariance" due to considerable restrictions needing to be imposed to achieve total invariance. The used a state propagation matrix, a matrix that is a function of the initial time and a given final time. When multiplying a state transition matrix with the array of initial conditions, the product is the array of conditions at the final time. The state transition matrix used by Breger and How included the effects of J_2 perturbations in the form of osculating elements. The drift produced was then multiplied by a weighted norm, allowing for a definition of more and less favorable drift components. The method also included a contribution due to the amount of fuel required to overcome the secular drift, once again allowing for the multiplication of a weighing value. Both of these values were used to create a cost function. This value was then optimized, resulting in the most desirable initial conditions for the given weighed values.

Special Inclinations from Genetic Algorithm

In addition, the results of this J_2 invariant method were used by Sabitini, et al (5:97-100). The method used a genetic algorithm with the refined initial conditions, established through use of the method determined by Alfriend and Schaub. The algorithm spanned the range of inclinations and used a value function to determine the method's accuracy at canceling out the secular drifts after 100 orbits. The paper

concluded that the method was fairly consistent and was able to reduce the secular effects of perturbation to approximately two thirds to one percent of the initial formation; however, for two angles and their complements the method was significantly more effective:

$$i=63.4^{\circ}; 116.6^{\circ}$$

$$i=49^{\circ}; 131^{\circ}$$

The first two angles are known as the critical inclinations, the inclinations where the secular drift of the argument of perigee is zero. The second pair has been labeled by the author as "special inclinations" continuing to reserve the previously established title of critical inclination for the previous pair.

Active Control

One method of overcoming the secular effects of perturbations was approached by William Weisel (10:74-78). The method included optimizing two-impulse control maneuvers on satellite formations by allowing the satellite to follow more natural dynamics. The method used a Floquet method of propagation that included fourteenth order geopotential as well as air drag and used the natural perturbation forces to aid in minimizing the amount of impulse required to maintain the cluster. However, the paper stated that the fuel required to maintain specific geometries would far exceed practicality and looked more at formations intent on maintaining relative distances. To contrast, this thesis will assume that certain aspects of the relative geometry are required and will try to obtain minimum drift rates while achieving those specifications.

Defining a Relative Orbit

The method of obtaining relative geometry between satellites starts with the declaration of the primary satellite. This satellite will be labeled the "chief" and the other satellites will be considered "deputies." For this thesis, a single deputy was considered; however, the concepts can be applied for multiple satellite formations. When describing the relative position, the most commonly used coordinate frame is Hill's frame. This frame is an orthogonal coordinate system whose origin is located at the chief's position. The *x*-axis is in the radial direction of the chief. The *y*-axis is in the direction of the chief's velocity, and the *z*-axis is normal to the chief's orbital plane with a right-handed orientation. In this coordinate frame a linear set of differential equations describing the relative motion was established by Hill as well as Clohessy and Wiltshire, with a slightly different orientation. Because these equations are much alike, the differential equations established are referred to as Hill's equations, Clohessy-Wiltshire (CW) equations, and Hill-Clohessy-Wiltshire (HCW) equations. In the simplest form these differential equations can be expressed as:

$$\begin{aligned} \ddot{x} - 2n\dot{y} - 3n^2 x &= 0 \\ \ddot{y} + 2n\dot{x} &= 0 \\ \ddot{z} + n^2 z &= 0 \end{aligned} \tag{1}$$

Where n is the mean motion of the chief's orbit and can be expressed as:

$$n = \sqrt{\frac{\mu}{a^3}} \tag{2}$$

This particular form of these differential equations is based on three assumptions. One is that the only acceleration is gravitational acceleration from a point mass. The second is the assumption of a circular chief orbit. The third is that the relative vector is

considerably smaller than the chief's position vector, allowing the second order terms to be neglected (9:282-285):

$$e_r = O\left(\frac{(r_d - r_c)^2}{r_c^{\,2}}\right) \tag{3}$$

It should be pointed out that these differential equations are independent of the deputy's position in *y*-direction. This means that for unperturbed motion, there are certain significant initial conditions:

$$X = \begin{vmatrix} x \\ y \\ z \\ \dot{x} \\ \dot{y} \\ \dot{z} \end{vmatrix} = \begin{bmatrix} 0 \\ y_0 \\ 0 \\ 0 \\ 0 \\ 0 \end{bmatrix} \tag{4}$$

The resulting relative motion for these initial conditions would be unchanged and has been used repeatedly due to its stable relative position. This particular formation is commonly referred to as the leader-follower formation. In addition to being invariant to displacements in the *y*-direction, the equations are also decoupled in the z-direction. Consider the following initial conditions:

$$X = \begin{vmatrix} x \\ y \\ z \\ \dot{x} \\ \dot{y} \\ \dot{z} \end{vmatrix} = \begin{bmatrix} 0 \\ y_0 \\ z_0 \\ 0 \\ 0 \\ \dot{z}_0 \end{bmatrix} \tag{5}$$

This would produce a relative orbit that is invariant in the *x* and *y* directions, while oscillating in the *z*-direction. Though it is possible for large oscillations in the *z*-direction

to make contributions in the negative *x* position, due to the deputy's position projected onto the chief's orbital plane, these linear differential equations do not account for this.

Defining ROE

Though Hill's frame coordinates accurately describe the relative position and velocity, much like Earth Centered Inertial (ECI) position and velocity vectors for a single satellite, these usually do not allow for a very good understanding of the relative orbit. To correct this inconvenience, the Relative Orbital Elements (ROE) were introduced by Lovell and Tragessor (3:2-4) . These orbital elements are defined by the following six equations:

$$\begin{aligned} a_e &= 2\sqrt{\left(\frac{\dot{x}}{n}\right)^2 + \left(3x + 2\frac{\dot{y}}{n}\right)^2} \\ x_d &= 4x + 2\frac{\dot{y}}{n} \\ y_d &= y - 2\frac{\dot{x}}{n} \\ \beta &= \text{atan2}\left(\dot{x}, 3nx + 2\dot{y}\right) \\ z_{\max} &= \sqrt{\left(\frac{\dot{z}}{n}\right)^2 + z^2} \\ \gamma &= \text{atan2}\left(nz, \dot{z}\right) - \beta \end{aligned} \tag{6}$$

Where atan2 is an inverse tangent function that puts the first term over the second term, it also uses the signs of each to eliminate quadrant ambiguity.

For a circular chief and a deputy with a matching period, the deputy would follow a two-by-one ellipse whose semi-major axis is in the direction of the chief's velocity vector and is designated by, a_e. The center of the two-by-one ellipse is located on the point (x_d, y_d). The angle β, represents the deputy's position on the ellipse. It is defined as the angle from the negative *x*-axis to the deputy's position projected on the chief's x-y

plane. For a circular chief this would correspond to the deputy's mean angle from its own perigee. The deputy's maximum displacement in the *z*-direction defines the element z_{max}. The angle γ is sometimes referred to as the relative ascending node, but is in fact opposite in sign to that angle. This angle represents the difference in the oscillation angle in the *z*-direction and the angle β. For further clarification, please refer to Figure 29 in Appendix B.

Linear Approach

One approach, to minimize the secular effects of J_2 perturbations, was used by Tragessor and Skrehart (8:1-15) and is one that I will refer to as the linear approach. The time rate of change of the orbital element differences was written in relative orbital parameters resulting in the following equations:

$$\begin{aligned}\delta(\dot{\mathrm{M}}+\dot{\omega}) = &-\frac{1}{2a}\left[3n+7C(1-\frac{3}{2}\sin^2 i)\eta+7C(\frac{5}{2}\cos^2 i-\frac{1}{2})\right]x_d \\ &+\frac{C}{8a^2}\left[3(1-\frac{3}{2}\sin^2 i)+\frac{4}{\eta}(\frac{5}{2}\cos^2 i-\frac{1}{2})\right]{a_e}^2 \\ &-\frac{C}{a}\cos i\sin i(3n+5)z_{\max}\cos\left[\theta-(\gamma+\beta)\right]\end{aligned} \tag{7}$$

$$\delta\dot{\Omega} = \frac{7C}{2a}\cos i\ x_d - \frac{C}{2\eta a^2}\cos i\ {a_e}^2 + \frac{C}{a}\sin i\ z_{\max}\cos\left[\theta-(\gamma+\beta)\right] \tag{8}$$

Where η and C are defined as:

$$\eta = (1-e^2)^{1/2} \tag{9}$$

$$C = \frac{3J_2{R_e}^2 n}{2a^2\eta^4} \tag{10}$$

Their previous work concentrated primarily on fixing the size of the relative orbit, a_e, and solving for the resulting semi-major axis shift, x_d, and out of planar motion, z_{max}

resulting in both of the equations producing zero secular changes. The resulting solution was incredibly effective at establishing invariance for co-planar orbits. However, when out of planar motion was introduced, the method was much less successful. By attempting to choose both a size a_e and fixing a magnitude of the out of planar motion, z_{max}, the two equations became over-constrained with the only apparent remaining variable being the difference in semi-major axis, x_d. This would suggest that the system of equations had no solution. Essentially, this required zeroing out two independent equations while only being able to adjust one variable. Upon removing the constraint on a_e, the system was still considerably constrained due to both equations' relative insensitivity to changes in a_e.

When an orbit was propagated for ten orbits without modification to the initial conditions, the corresponding in-plane drift was approximately fourteen meters per orbit. With an out of plane drift of approximately 5 cm per orbit, the decision was made to use period matching to cancel the drift in the orbital direction. This reduced the drift in the y direction to 1.4 meters per orbit.

III. Methodology

This work began by establishing how the initial conditions are defined. Afterwards the secular effects of the J_2 perturbation on the ROE were determined, and the conditions for establishing invariance were defined. Then, the linear method presented Tragesser and Skrehart was modified and analyzed. Finally, a non-linear method was introduced, and the accuracy was determined through numerical integration.

Determining Initial Conditions

During the course of this thesis the initial conditions for the chief will be set. These initial conditions will be given in classical orbital elements:

$$IC = \begin{bmatrix} a \\ e \\ i \\ \Omega \\ \omega \\ \nu \end{bmatrix} \tag{11}$$

Schaub (7:606-611)6. Schaub, H. and Alfriend, K. T., "J2 Invariant Relative Orbits for Spacecraft Formations," Flight Mechanics Symposium, (Goddard Space Flight Center, Greenbelt, Maryland), January 18-20, 2002, Paper No. 11, pp. 77-95

7 currently has a method for converting orbital elements and orbital element differences into a relative position vector in Hill's frame. The process begins by defining two arrays that contain the chief and deputy's initial conditions in the following orbital elements:

$$r_{oe} = \begin{bmatrix} a \\ \theta \\ i \\ q_1 \\ q_2 \\ \Omega \end{bmatrix} \tag{12}$$

Where the elements q_1, q_2, and θ have been used to cancel out the singularity in the argument of perigee for a zero eccentricity orbit, and have been defined as:

$$\begin{aligned} q_1 &= e\cos\omega \\ q_2 &= e\sin\omega \\ \theta &= \omega + \nu \end{aligned} \tag{13}$$

Due to small eccentricities the true anomaly, υ, will be approximated with the mean anomaly, M. The symbol δe_{oe} in Eq. (16) would represent the array containing the differences in orbital elements between the deputy and the chief:

$$\delta e_{oe} = r_{doe} - r_{coe} \tag{14}$$

The values in this vector are then described as follows:

$$\delta e_{oe} = \begin{bmatrix} \delta a \\ \delta\theta \\ \delta i \\ \delta q_1 \\ \delta q_2 \\ \delta\Omega \end{bmatrix} \tag{15}$$

This conversion is in the form of:

$$X = [A]\delta e_{oe} \tag{16}$$

The transformation matrix [A] is given with perturbations, by Gim (2:962). A version without the perturbation terms can be found in Luck (4:1) and is seen in Appendix A. The vector output of this expression is a 6x1 array that contains both the relative position and velocity in Hill's frame:

$$X = \begin{bmatrix} x \\ y \\ z \\ \dot{x} \\ \dot{y} \\ \dot{z} \end{bmatrix} \tag{17}$$

Though the state transition matrix, [A], allows for non-circular chief orbits, the complexity of the equations reduces the understanding of the resulting equations. Therefore, the transformation matrix was significantly simplified with the assumption of a circular chief orbit. The resulting vectors in Hill's frame are as follows:

$$\begin{aligned} x &= \delta a - a\cos\theta\delta q_1 - a\sin\theta\delta q_2 \\ y &= a\delta\theta + a\cos i\delta\Omega \\ z &= a\sin\theta\delta i - a\cos\theta\sin i\delta\Omega \\ \dot{x} &= an\sin\theta\delta q_1 - an\cos\theta\delta q_2 \\ \dot{y} &= -\frac{3n}{2}\delta a + 2an\cos\theta\delta q_1 + 2an\sin\theta\delta q_2 \\ \dot{z} &= an\cos\theta\delta i + an\sin i\sin\theta\delta\Omega \end{aligned} \tag{18}$$

James Luck (4:1-4) used these equations and substituted them into Eq. (6) to produce the following expressions, which can be used to transform small changes in COE to ROE:

$$\begin{aligned} a_e &= 2a\sqrt{(\delta q_1)^2 + (\delta q_2)^2} \\ x_d &= \delta a \\ y_d &= a\delta\theta + a\cos i\delta\Omega - 2a(\sin\theta\delta q_1 - \cos\theta\delta q_2) \\ z_{\max} &= a\sqrt{(\delta i)^2 + (\sin i\delta\Omega)^2} \\ \beta &= \text{atan2}(\sin\theta\delta q_1 - \cos\theta\delta q_2, \cos\theta\delta q_1 + \sin\theta\delta q_2) \\ \gamma &= \text{atan2}(\sin\theta\delta i - \cos\theta\sin i\delta\Omega, \cos\theta\delta i + \sin\theta\sin i\delta\Omega) - \beta \end{aligned} \tag{19}$$

These expressions may then be used to determine the contributions due to the secular effects of the orbital elements and orbital element differences.

Defining ROE Invariance

Though Eq. (19) was established with an orbital element s set specifically designed to minimize singularities near zero eccentricity, it is easier to understand the perturbation effects when the expressions are written in classical orbital elements and classical orbital element differences. After simplifying the expressions to reflect classical orbital elements and orbital element differences the equations become:

$$\begin{aligned} a_e &= 2a\delta e \\ x_d &= \delta a \\ y_d &= a\delta\theta + a\cos i\delta\Omega - 2a\delta e\sin(\theta-\omega_d) \\ z_{\max} &= a\sqrt{(\delta i)^2 + (\sin i\delta\Omega)^2} \\ \beta &= \text{atan2}\left(\sin(\theta-\omega_d),\cos(\theta-\omega_d)\right) = (\theta-\omega_d) \\ \gamma &= \text{atan2}\left(\sin\theta\delta i - \cos\theta\sin i\delta\Omega, \cos\theta\delta i + \sin\theta\sin i\delta\Omega\right) - \beta \end{aligned} \tag{20}$$

It is clear to see that one of the deputy's classical orbital elements, the argument of perigee, remains in the equations; fortunately, this allows for an easier understanding of the secular drift of the ROE containing that element.

It is clear to see that with the circular chief the ROE a_e and x_d will not experience secular drift due to purely periodic perturbations in the semi-major axis and eccentricities. In the equation for y_d, the periodic effects of $a\delta\theta$ and $-2a\delta e\sin(\theta-\omega_d)$ are equal and opposite for unperturbed dynamics. This is easier to spot when replacing $a\delta\theta + a\cos i\delta\Omega$ with y and by replacing $-2a\delta e\sin(\theta-\omega_d)$ with $-a_e\sin(\beta)$.

$$y_d = y - a_e\sin\beta \tag{21}$$

Therefore, in order to cancel out secular perturbations in y_d it is essential to minimize the drift rates in y. It can be seen that the only secularly affected components of y are due to secular contributions in the form of $\delta\dot{\theta}$ and $\delta\dot{\Omega}$. Therefore, by matching the secular drift rates in the argument of latitude and the longitude of the ascending node, this ROE will

not vary secularly. In addition, it can be seen that z_{max} is also a function of $\delta\dot{\Omega}$ and that minimizing this will also establish reduced secular effect in z_{max}. This has been shown time and again for invariant formations and could be expected.

In addition, in order to establish true invariance in the ROE, other terms would also have to be taken into consideration. Canceling out secular perturbations found in β and γ would require a different definition. Due to the rapid rate of change of β, an invariant drift rate could be defined by stating a desired β for a given angle θ. In order to maintain this desired initial condition, the secular drift of the deputy's argument of perigee would have to be zero. This is possible, but would require the deputy to be located at the critical inclination.

If the secular drift in β would be considered zero when there are no longer any affects of J_2, then the following condition would have to be met:

$$(\dot{M}_c + \dot{\omega}_c) = \dot{\omega}_d \tag{22}$$

It can be seen that in order for this and $\delta\dot{\theta}$ to both be zero, the secular drift rate of the deputy's mean anomaly would have to be zero. This would also impose a restriction on the deputy's inclination; now requiring a 54.7°. Although both of these would be possible, the imposed inclination restrictions would severely restrict the orbits. Therefore, canceling out the secular effects in the angle β will not be required to establish invariance.

Furthermore, because γ is equal to a function of $\delta\Omega$ minus β; once $\delta\dot{\Omega}$ is near zero the value for γ will have a rate of change equal and opposite to that of β. Therefore, with a circular chief a J_2 invariant relative orbit will require zero secular drift in y_d and z_{max}.

Defining Initial Conditions

The purpose of this thesis is to take a set of initial conditions for the chief and a desired set of ROE and adjust the ROE slightly in order to reduce the secular effects of the J_2 perturbation. The method will then be verified with numerical integration. The verification process will begin by using the ROE to determine the orbital element differences. The classical orbital elements for the deputy are then calculated. Both sets of orbital elements are then individually transferred into vectors in the Earth Centered Inertial (ECI) frame. These were then integrated using a fourth order numerical integrator. The output was then converted back into classical orbital elements, and the relative vectors were then calculated in Hill's frame. The ROE were then calculated for each time step.

Due to the effects of the J_2 perturbation being inversely proportional to the semi-major axis, satellites in Low Earth Orbit will be analyzed. The primary semi-major axis used in this thesis is 7000 km. This orbit should be small enough to produce non-trivial effects of J_2, while still remaining high enough that the effects of J_2 will remain the dominant perturbation. The first case will consider a chief orbit with an inclination of thirty degrees. This inclination has been chosen because it is near the 28.5° launch latitude of Cape Canaveral and it has not shown any traits that would render it an exceptional case. This case takes into consideration both the effects due to changes in eccentricity, as well as out of planar motion. The unmodified set of initial conditions is as follows:

Chief orbit	Desired ROE
$a = 7000$ km	$a_e = 500$ m
$e = 0$	$x_d = 0$ m
$i = 30$	$y_d = 0$ m
$\Omega = 0^\circ$	$\beta = 0^\circ$
$\omega = 0^\circ$	$\gamma = 0^\circ$
$\nu = 0^\circ$	$z_{\max} = 500$ m

Figure 1 is a plot of the chief's position, (0,0), and the deputy's relative orbit about that position. In the graph the nearly horizontal line represents the direction of the orbit travel. The nearly vertical line points in the negative x direction representing the direction of the center of the chief's orbit and terminates at approximately the deputy's initial position. In Figure 2 the chief is again located at (0, 0) and the deputy's projection onto the x-y orbital plane follows the outside trajectory beginning at (0, -250m) and proceeding in the anti-clockwise direction. Also plotted, beginning at (0, 0) and drifting in the negative y direction, is x_d vs. y_d.

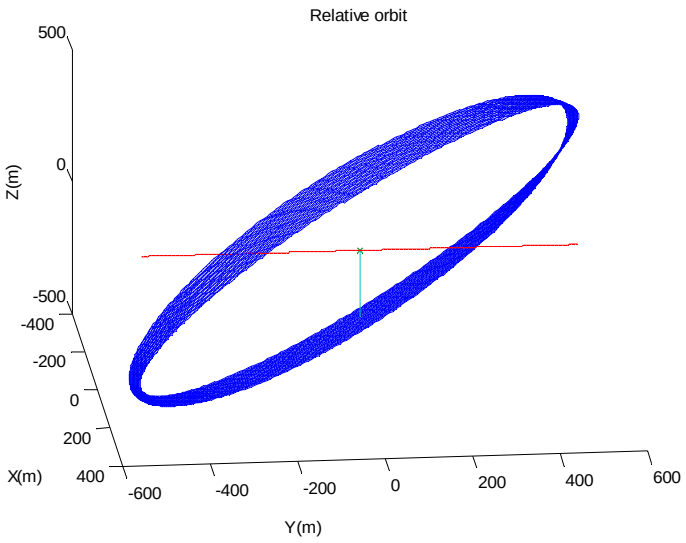

Figure 1: 3-Dimensional J_2 Drift for Uncorrected IC

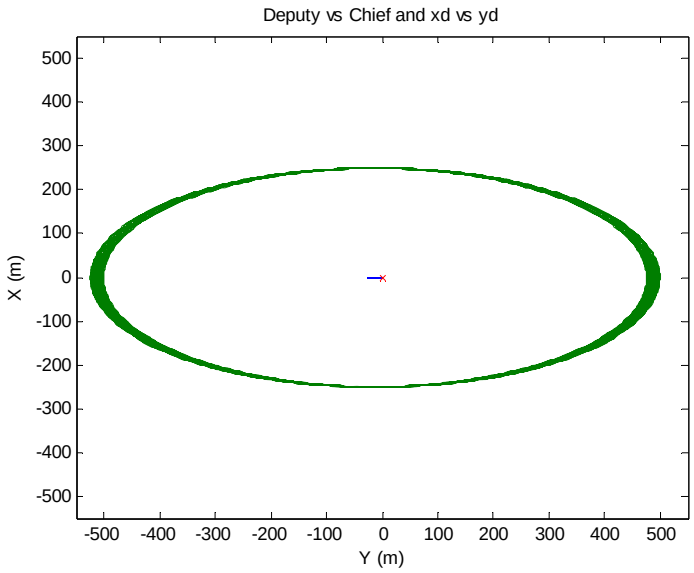

Figure 2: Orbital Plane J_2 Drift for Uncorrected IC

The figures above allow for better understanding of the relative motion, as well as a slightly better understanding of the effects of the secular drifts and. In Figure 2 the *x* and *y* components of the data have been plotted in the chief's orbital plane. It is apparent in this graph that this method produces the classic two-by-one ellipse that defines a relative orbit about a circular chief orbit. Though it is difficult to determine the magnitude of the secular drift from this graph, it is apparent that a secular drift is present and the plot of (x_d,y_d) shows that the deputy is drifting in the negative *y*-direction. To allow for a better determination of the rates of change, the following figures plot the *y*-position in meters vs. time in orbits.

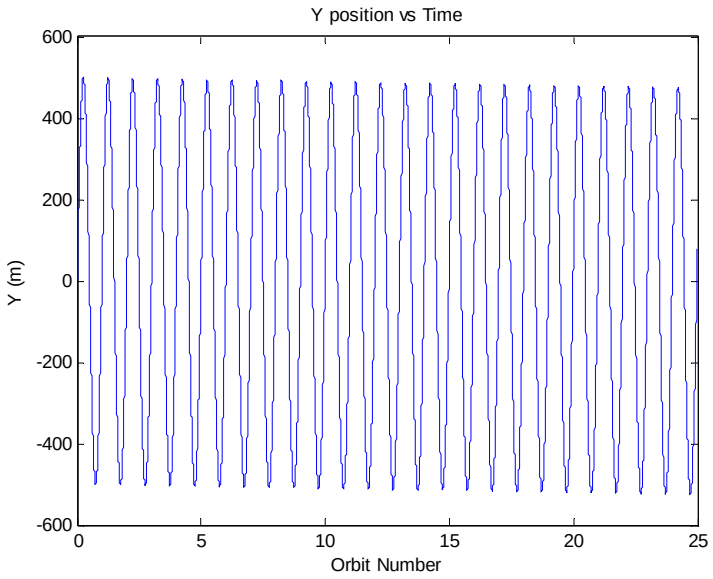

Figure 3: Relative Y-Position vs. Time for Uncorrected IC

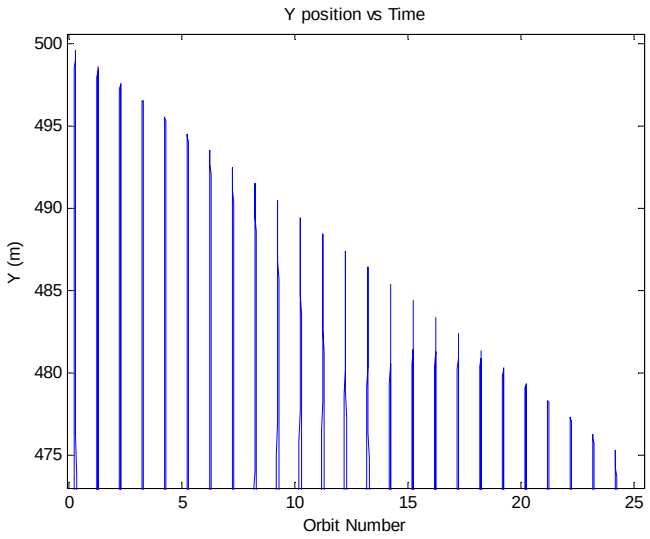

Figure 4: Maximum Displacement in Y-Direction for Uncorrected IC

From Figure 3 it is apparent that the primary motion in the *y*-direction is a periodic oscillation. However, because of the scale it is hard to distinguish the secular effects that have been introduced due to perturbation accelerations. Figure 4 is a close up of the maximum displacements in the *y*-direction. The figure shows that there is a

negative drift of approximately negative one meter per orbit. Likewise the following two graphs plot the displacement in the *z*-direction vs. time.

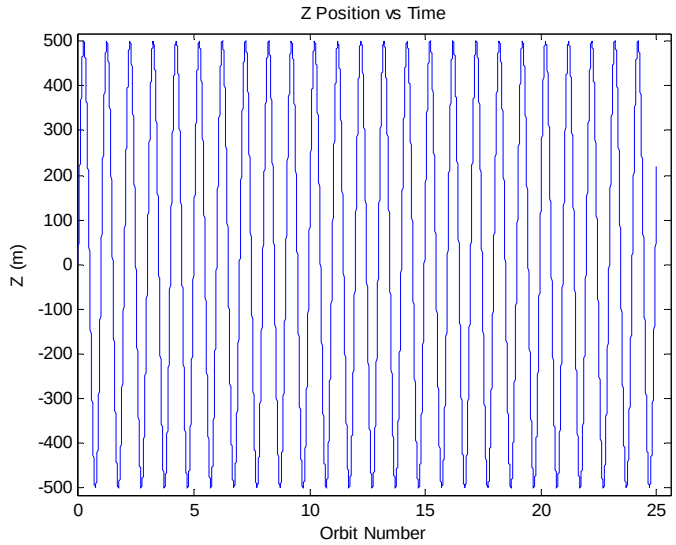

Figure 5: Out of Plane Position vs. Time

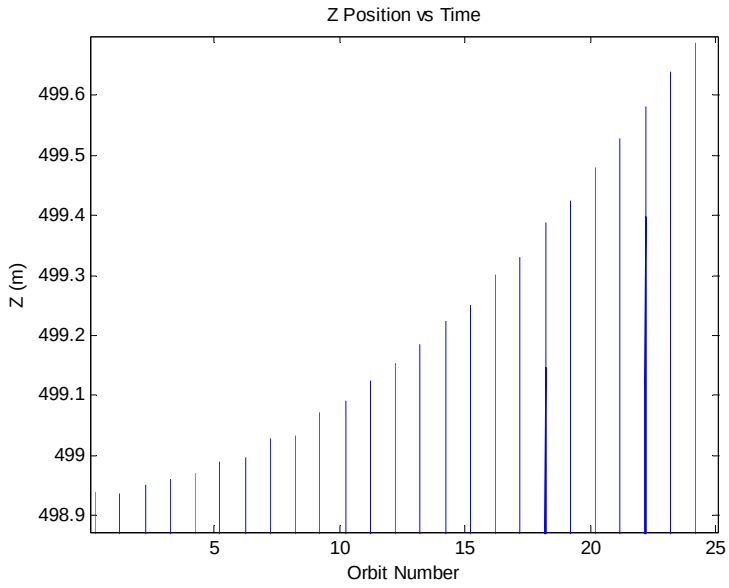

Figure 6: Maximum out of Plane Position vs. Time

Once again, Figure 5 shows a dominant harmonic oscillation in the *z*-direction; however, the scale in Figure 6 allows for a better understanding of the drift in the *z*-direction. This drift is nonlinear, increasing about 70 cm over 25 orbits.

Pure Out-of-Plane Relative Motion

In the event that the relative motion desired is a pure oscillation in the *z*-direction, the value of a_e will be set to zero. This will cause both β and γ to lose definition, as both become a function of zero divided by zero. However, because this singularity exists in the transformation from Hill's Frame components into ROE, declaration of these values will produce legitimate initial conditions in Hill's frame that can be propagated to determine the relative motion.

This relative motion would include a harmonic oscillation in the *z*-direction that intersects the chief's orbital plane at (y_d, x_d). Therefore, in order for the initial conditions to be more realistic this case will include a non-zero y_d to prevent a collision with the chief satellite. However, due to previously established independence to displacements in the *y*-direction this will not affect the stability of the relative orbit.

The initial conditions have been established as follows:

Chief orbit	Desired ROE
$a = 7000$ km	$a_e = 0$ m
$e = 0$	$x_d = 0$ m
$i = 30^\circ$	$y_d = -25$ m
$\Omega = 0^\circ$	$\beta = 0^\circ$
$\omega = 0^\circ$	$\gamma = 0^\circ$
$\nu = 0^\circ$	$z_{\max} = 500$ m

These initial conditions were numerically propagated and can be seen in Figures 7 and 8.

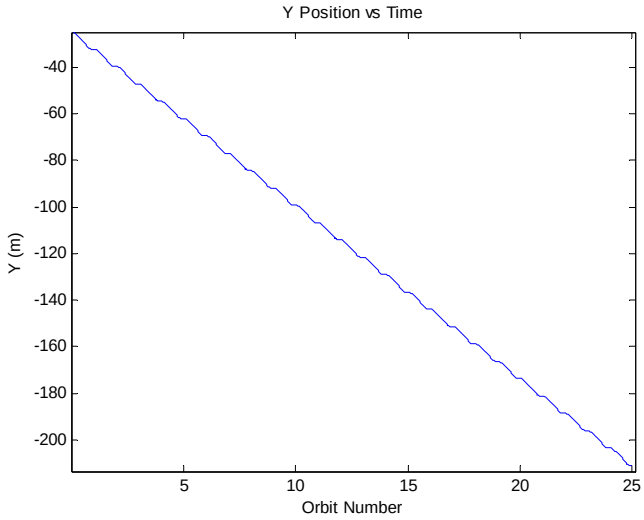

Figure 7: Maximum Displacement in Y-Direction

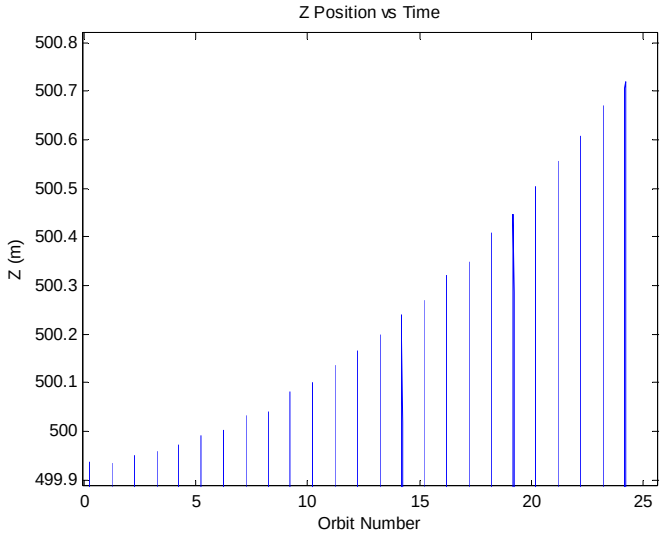

Figure 8: Maximum out of Plane Position vs. Time

In Figure 7, it can be seen that it is no longer necessary to scale the figure in order to determine the secular drift in the *y*-direction, due to the absence of the large harmonic oscillations that were present for a_e=500 m. This figure also shows a significant amount of secular drift in the orbital direction, approximately -7 meters per orbit.

Figures 6 and 8 show that in both cases, the drift in the z-direction appears parabolic. This is partly because the primary contribution to z_{max} is due to a difference in inclinations. Given the time derivative of z_{max}:

$$\frac{d(z_{\max})}{dt} = \frac{a \sin^2 i \delta\Omega \delta\dot{\Omega}}{\sqrt{(\delta i)^2 + (\sin i \delta\Omega)^2}} \tag{23}$$

For $(\delta i)^2 >> (\sin i \delta\Omega)^2$, the equation is approximately equal to:

$$\frac{d(z_{\max})}{dt} \approx \frac{a \sin^2 i \delta\Omega \delta\dot{\Omega}}{|\delta i|} \tag{24}$$

With a relatively constant value of $\delta\dot{\Omega}$ the value $\delta\Omega$ would increase linearly. Therefore Eq. (24) would increase linearly, resulting in parabolic growth of z_{max}. This would be indicative of a chief orbit with fairly low inclination, in which much of the out of plane motion is due to the difference in inclination as opposed to the right ascension of the ascending node. This is the case with the two previous scenarios, and helps explain the growth of z_{max} in Figures 6 and 8.

In the event that $(\sin i \delta\Omega)^2 >> (\delta i)^2$ the equation can be approximated as:

$$\frac{d(z_{\max})}{dt} \approx a \sin i \delta\dot{\Omega} \tag{25}$$

This equation would produce linear drift that would be expected due to secular effects. This would represent a chief orbit that is near polar, where most of the out-of-plane motion is due to difference in the right ascension of the ascending node. In both cases, a zero secular drift in the difference in the longitude of the ascending node would result in zero rate of change of z_{max}. Therefore, the secular drift rate of the difference in the longitude of the ascending nodes will be analyzed in more depth.

Secular Expansion

The equation for the secular drift in the differences of the longitude of the ascending node is as follows:

$$\delta\dot{\Omega} = \left(-\frac{3J_2 R_e^{\,2} n_d}{2a_d^{\,2}(1-e_d^{\,2})^2}\cos i_d \right) - \left(-\frac{3J_2 R_e^{\,2} n_c}{2a_c^{\,2}(1-e_c^{\,2})^2}\cos i_c \right) \tag{26}$$

After including the assumption of circular chief orbit and writing strictly as a function of the chief's orbital elements and the orbital element differences the equation becomes:

$$\delta\dot{\Omega} = \left(-\frac{3J_2 R_e^{\,2} \mu^{1/2}}{2(a+\delta a)^{7/2}(1-\delta e^2)^2}\cos(i+\delta i) \right) - \left(-\frac{3J_2 R_e^{\,2} \mu^{1/2}}{2a^{7/2}}\cos i \right) \tag{27}$$

Because the orbital element differences are considerably smaller than the terms they are grouped with, the expressions containing the differences can be expanded about the dominant value. After performing the expansions and combining the higher order terms, the expression becomes:

$$\begin{aligned}\delta\dot{\Omega} = {} & \frac{-3J_2 R_e^{\,2}\mu^{1/2}}{2a^{7/2}}\left(1-\frac{7\delta a}{2a}+O\left(\frac{\delta a^2}{a^2}\right)\right)(1+2\delta e^2+O(\delta e^4))\left(\cos i-\sin i\,\delta i+\frac{\cos i\,\delta i^2}{2}+O(\delta i^3)\right) \\ & +\frac{J_2 R_e^{\,2}\mu^{1/2}}{2a^{7/2}}\cos i\end{aligned} \tag{28}$$

In order to better understand the accuracy of the expression it would be worthwhile to consider the approximate order of magnitude of the higher order terms. For a semi-major axis of around 7000 km, in order to produce a z_{max} equal to or less than 5km the maximum δi will be on the order of 10^{-4}. Likewise, for an a_e on the order of 1km, the resulting δe will be on the order of 10^{-5}. Also, because secular drift due to differences in mean motion is highly dependent on differences in semi-major axis, J_2 invariance will often require δa smaller than 10^{-4} km. Therefore, higher order terms inside the parenthesis will be on the order of 10^{-12} radians per second. The resulting

round off error would create a secular drift of z_{max} on the order of millimeters per orbit. After cancellation and prioritizing by approximate maximum orders of magnitude the equation becomes:

$$\delta\dot{\Omega} = \frac{-3J_2R_e^{\,2}n}{2a^2}\left(\sin i\ \delta i + \frac{\cos i\ \delta i^2}{2} + 2\cos i\ \delta e^2 - \cos i\frac{\delta a}{a} + H.O.T.\right) \tag{29}$$

Once again, if a 1 km z_{max} was created strictly with a change in inclination, the first term could be on the order of 10^{-4}, whereas the remaining terms would be approximately four orders of magnitude smaller. This suggests that the largest step towards establishing J_2 invariance of this orbital element difference is to minimize the difference in the inclinations. However, Eq. (20) shows that the magnitude of the out of planar motion, z_{max}, is created by a combination of δi and $\delta\Omega\sin i$. Therefore, for any chief orbit without a near zero inclination this would not limit z_{max}; this would only limit the contribution resulting from the difference in inclinations.

Linear Approach

With this idea in mind, the linearizations put forth by Tragesser and Skrehart were then taken into consideration. Previous work has shown that these produce practical results for co-planar orbits; however, when out-of-planar motion is introduced the method becomes much less successful due to the sensitivities in the equation to small changes in z_{max}. However, if it was possible to nearly zero out the coefficients of z_{max} the equations would become much less sensitive to out-of-plane motion and it would be possible to re-establish the stability shown for co-planar orbits. Therefore, the coefficients of z_{max} will be considered in more depth:

$$\delta(\dot{\mathrm{M}} + \dot{\omega}) = f_1(C_{oe}, x_d, a_e{}^2) - \frac{C}{a}\cos i \sin i(3n+5) z_{\max} \cos\left[\theta - (\gamma + \beta)\right]$$
$$\delta\dot{\Omega} = f_2(C_{oe}, x_d, a_e{}^2) + \frac{C}{a}\sin i \; z_{\max} \cos\left[\theta - (\gamma + \beta)\right] \tag{30}$$

Two terms that are present in both coefficients of z_{max} are a^{-1} and sin$i$. Though it would be possible to increase the magnitude of the variable a to the point where both equations become nearly independent of z_{max}, and even more possible to choose a chief with a zero inclination, the resulting orbits would be considerably constrained. There is however another term that shows up in both equations:

$$\cos\left[\theta - (\gamma + \beta)\right] \tag{31}$$

This term is bound between one and negative one. In theory, if it is possible to choose the correct combination of θ, γ, and β it should be possible to nearly zero out the contributions of z_{max} and re-establish the same stability displayed for co-planar formations.

Because γ is the angular difference between the oscillation angle in the z-direction and the position-based angle β, $(\gamma + \beta)$ simplifies to the angle of the oscillation in the z-direction and will be labeled as γ_z.

$$\gamma_z = a\tan 2\left(nz, \dot{z}\right) = \gamma + \beta \tag{32}$$

$$\cos\left[\theta - (\gamma + \beta)\right] = \cos(\theta - \gamma_z) \tag{33}$$

These angles left inside the parenthesis are increasing at a given frequency. For $\dot{y}_d = 0$ both angles would increase at a rate equal to the mean motion. Resulting difference is relatively constant. Because there are now two components that are functions of relative orbital elements, it is possible to fix z_{max} and replace the expression $\cos\left[\theta - (\gamma + \beta)\right]$ with a new variable z_γ.

$$z_\gamma = \cos(\theta - \gamma_z) \tag{34}$$

Furthermore, if a_e^2 is also chosen, two of the main components of the relative geometry have been fixed; the magnitude of the two-by-one ellipse, a_e^2, and the magnitude of the out of plane motion, z_{max}. By setting the difference in drift rates equal to zero and bringing the now constant contribution of a_e^2 to one side the expression can be written as:

$$[A] \begin{pmatrix} x_d \\ z_\gamma \end{pmatrix} = [D] a_e^{\,2} \tag{35}$$

Where:

$$\begin{aligned} [A] &= \begin{bmatrix} -\frac{1}{2a}\left[3n + 7C(1-\frac{3}{2}\sin^2 i)\eta + 7C(\frac{5}{2}\cos^2 i - \frac{1}{2})\right] & -\frac{C}{a}\cos i \sin i(3n+5) z_{\max} \\ \frac{7C}{2a}\cos i & \frac{C}{a}\sin i \; z_{\max} \end{bmatrix} \\ [D] &= \begin{bmatrix} -\frac{C}{8a^2}\left[3(1-\frac{3}{2}\sin^2 i) + \frac{4}{\eta}(\frac{5}{2}\cos^2 i - \frac{1}{2})\right] \\ \frac{C}{2\eta a^2}\cos i \end{bmatrix} \end{aligned} \tag{36}$$

This gives a closed form solution for both z_γ and x_d in the form:

$$\begin{pmatrix} x_d \\ z_\gamma \end{pmatrix} = [A]^{-1} [D] \, a_e^{\,2} \tag{37}$$

Note that since z_γ is a function of the sum $\gamma + \beta$, we can arbitrarily select β and still satisfy the conditions by choosing the correct γ to satisfy Eq. (32). This means that for a given z_{max} and a_e the full solution is now a solution set whose relative positions lay on the two-by-one ellipse offset by the chief's orbital plane by a distance of $z_{\max} \sin \gamma_z$.

This would allow for multiple satellites to occupy the same solution set, with different angles β and γ but still maintaining the same z_γ. In addition, because the cosine function is even, both a positive and negative angle γ_z fulfill the requirements for z_γ. Combine this with y_d independence, and this allows for β, z_{max}, a_e, and y_d to be set arbitrarily. This allows the ROE x_d and γ to be adjusted in order to establish the desired invariance.

Analysis of Linear Approach for Circular Deputy

To investigate the effectiveness of this method to reduce the effects of the J_2 perturbations on a formation, numerical simulations were performed. This method will include the initial conditions established previously for a pure oscillation in the *z*-direction. Once again, this initial condition causes β and γ to lose physical interpretation and become undefined; however, because z_γ remains defined, the initial value of β will once again be set to zero and the value for the initial condition of γ will be computed.

Chief orbit:	Desired ROE:
$a = 7000$ km	$a_e = 0$ m
$e = 0$	$x_d = 0$ m + TBD Adjustment
$i = 30^\circ$	$y_d = -25$ m
$\Omega = 0^\circ$	$\beta = 0^\circ$
$\omega = 0^\circ$	$\gamma =$ TBD
$\nu = 0^\circ$	$z_{\max} = 500$ m

After substituting these values into the previously established equations the initial conditions are determined to be:

$$\begin{pmatrix} x_d \\ z_\gamma \end{pmatrix} = \begin{bmatrix} 0 \text{ km} \\ 0 \end{bmatrix} \tag{38}$$

The z_γ allowed for a $\gamma = \pm 90°$. For this case the positive value of gamma will be chosen. The resulting initial conditions are as follows:

Chief orbit:	Desired ROE:
$a = 7000$ km	$a_e = 0$ m
$e = 0$	$x_d = 0$ mm
$i = 30^\circ$	$y_d = -25m$
$\Omega = 0^\circ$	$\beta = 0^\circ$
$\omega = 0^\circ$	$\gamma = 90^\circ$
$\nu = 0^\circ$	$z_{\max} = 500$ m

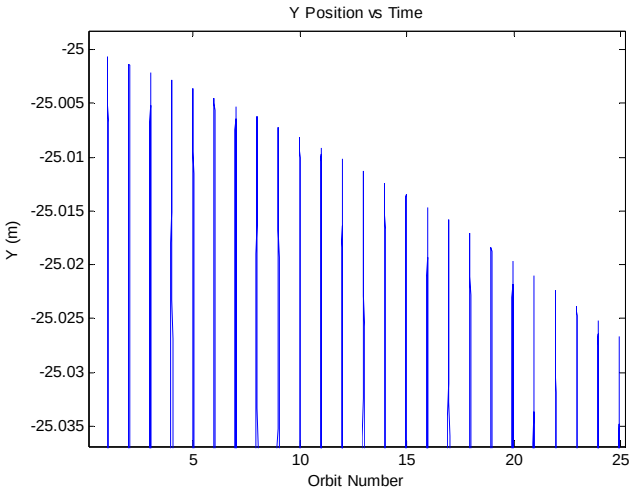

Figure 9: Maximum Displacement in *Y*-direction

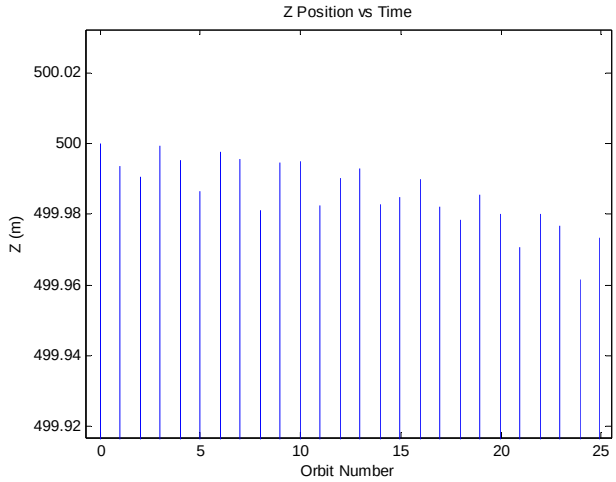

Figure 10: Maximum Displacement in *Z*-direction

As Figure 9 shows, this method is highly successful at reducing the secular drift in the *y*-direction. The resulting secular drift is approximately -1 mm/orbit as opposed to over -7 m/orbit drift seen in Figure 7. Likewise, Figure 10 also shows a drift multiple times smaller than the drift observed in Figure 8.

It is also worth mentioning that the apparently trivial solution seen in Eq. (38) allows for a slight amount of understanding of the modifications to the initial linear method. Had the system of equations been used as they were previously in Eqs. (7) and (8), to solve z_{max} and x_d, the solution set would have required a zero maximum displacement in the *z*-direction. This would limit the solution to a leader-follower formation observed in Eq. (4). However, by solving for z_γ the solution now allows for displacements in the *z*-direction, resulting in the initial conditions previously mentioned in Eq. (5).

Analysis of Linear Approach for Non-Circular Deputy

Though this method produces accurate results for near zero a_e, for moderate a_e this method produces much less desirable results. The following initial conditions are identical to the previously chosen initial conditions with the exception of a 500 meter a_e:

For a given chief orbit:	Desired ROE:
$a = 7000$ km	$a_e = 500$ m
$e = 0$	$x_d = 0$ + TBD Correction
$i = 30^\circ$	$y_d = 0m$
$\Omega = 0^\circ$	$\beta = 0^\circ$
$\omega = 0^\circ$	$\gamma =$ TBD
$\nu = 0^\circ$	$z_{\max} = 500$ m

For this particular formation Eq. (37) establishes x_d = -0.031 mm and $\gamma = 89.996^\circ$. The graph below shows the projection of the deputy's orbit projected onto the chief's orbital plane.

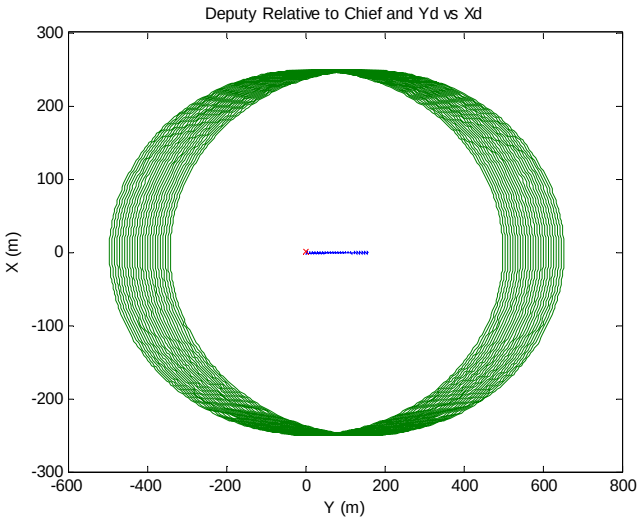

Figure 11: Relative Orbit from Linear Results a_e of 500 m

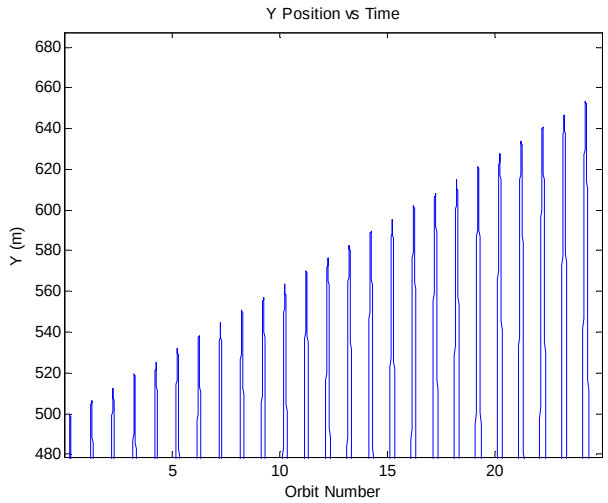

Figure 12: Maximum Positive Displacement in *Y*-direction from Linear Results

The Figures 11 and 12 clearly show that y_d is drifting in the positive y-direction at a rate of over 5 meters per orbit. A second run with x_d = 0m gave almost identical results.

When also considering that positive displacements in x_d result in negative drifts, it can safely be deducted that x_d should have been larger in magnitude and positive. However, this case still shows that this method is still highly successful at reducing the secular drift in z_{max}, as shown in Figure 13.

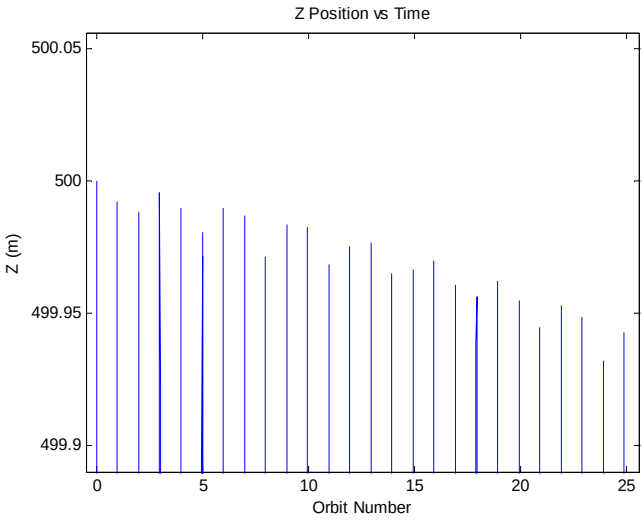

Figure 13: Maximum Displacement in *Z*-Direction

Due to the less than desirable accuracy of the linear solver, a more accurate method of determining x_d was required.

Single Variable Nonlinear Solver

Since the linear approach was unable to cancel out the secular drift in the orbital direction, a nonlinear approach was taken to find values of x_d and γ which would result in:

$$\dot{y}_d = 0$$
$$\dot{z}_{\max} = 0$$

In order to determine $\frac{\delta \dot{y}_d}{\delta x_d}$ the initial conditions from the linearization were numerically propagated for four orbits. The time and position of the maximum

displacement in the *y*-direction were recorded and run through a linear best fit to help reduce error. The slope that was produced through best fit was considered the secular drift in the *y*-direction, $\dot{y}_d$. This was repeated for a second x_d. The difference in the slopes produced by the linear best fit, over the differences in x_d was and $\frac{\delta \dot{y}_d}{\delta x_d}$ was determined. The secular drift $\dot{y}_{d0}$ was the error and the new x_d was calculated:

$$\begin{aligned} e_r &= \dot{y}_{d0} \\ \dot{y}_d &= e_r + \frac{\delta \dot{y}_d}{\delta x_d} \delta x_d \end{aligned} \tag{39}$$

Setting $\dot{y}_d$ equal to zero and solving for x_d produces:

$$\begin{aligned} \delta x_d &= -e_r \frac{\delta x_d}{\delta \dot{y}_d} \\ x_d &= \delta x_d + x_{d0} \end{aligned} \tag{40}$$

Due to non-linearity in the equation this method had to be repeated until the drift rate was within desired tolerances. The x_d was then re-introduced into the secular drift rate of $\delta\dot{\Omega}$ to solve for γ.

Thirty Degree Inclination

After using the non-linear approach to the previous set of initial conditions resulted in the following relative orbit:

For a given chief orbit:	Desired ROE:
$a = 7000$ km	$a_e = 500$ m
$e = 0$	$x_d = 67.61$ cm
$i = 30^\circ$	$y_d = 0$ m
$\Omega = 0^\circ$	$\beta = 0^\circ$
$\omega = 0^\circ$	$\gamma = 89.972^\circ$
$\nu = 0^\circ$	$z_{\max} = 500$ m

The resulting relative orbit is shown in Figure 14.

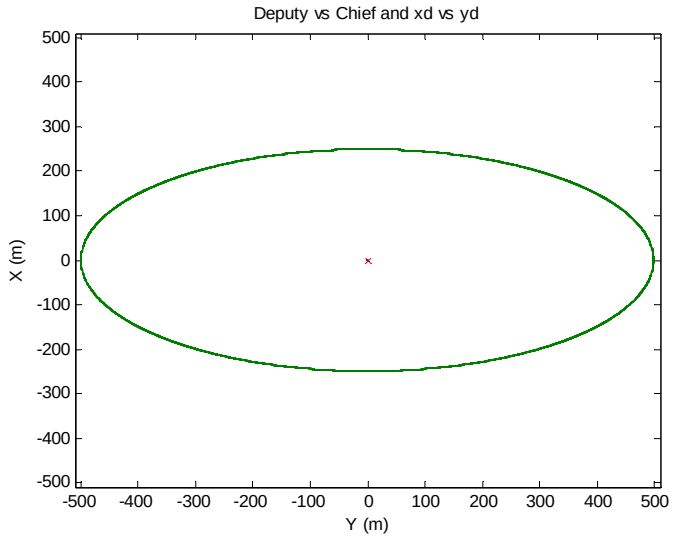

Figure 14: Corrected Relative Orbit with 30° Inclination Chief

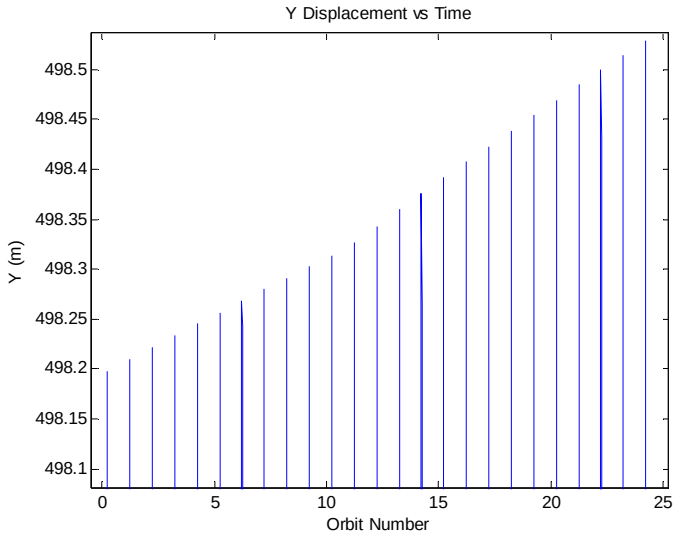

Figure 15: Maximum Y Displacement vs. Time with 30° Inclination Chief

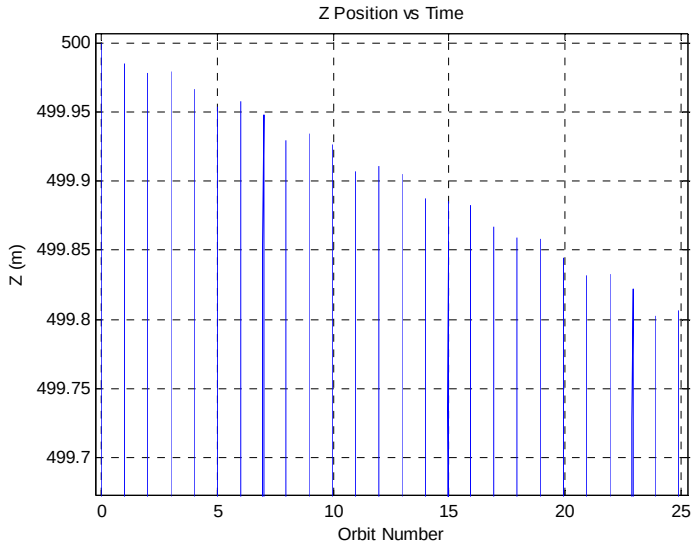

Figure 16: Maximum Z Displacement vs. Time with 30° Inclination Chief

It can be seen from Figures 14 and 15 that this method is successful at significantly reducing the secular drift rate in the orbital direction, while Figure 16 shows that the method has also maintained accuracy in the out-of-plane direction. This case was for verification purposes only; therefore, the iterations were stopped at an accuracy of approximately 1 cm drift per orbit in the *y*-direction. When the method is used to maximize accuracy the iterations will continue until the secular drift in the orbital direction is less than 1 mm per orbit.

Two Variable Nonlinear Method

Although the single variable method is effective at reducing the secular effects of the J_2 perturbation, it is possible to further reduce the secular drift in the out-of-plane direction by expanding the non-linear method to solve for both variables simultaneously. The method begins with a propagation of the initial conditions for the previously established four orbits. The secular drifts in the *y* and *z* directions are determined. Afterwards the obit was propagated once again with only a small change in x_d and then

again with only a small change in γ. The resulting rates of change of the maximum displacements in the *y* and *z* directions were once again determined. These values were then used to express the differences in the rates of change of the error over the differences in the initial conditions.

$$\begin{bmatrix} \frac{\Delta \dot{y}_d}{\Delta x_d} & \frac{\Delta \dot{y}_d}{\Delta z_\gamma} \\ \frac{\Delta \dot{z}_{\max}}{\Delta x_d} & \frac{\Delta \dot{z}_{\max}}{\Delta z_\gamma} \end{bmatrix} \tag{41}$$

The error was then defined as:

$$e_r = \begin{pmatrix} \dot{y}_{d0} \\ \dot{z}_{\max 0} \end{pmatrix} \tag{42}$$

The initial conditions for the next iteration were then determined by the following equation:

$$\begin{pmatrix} x_d \\ z_\gamma \end{pmatrix} = -\begin{bmatrix} \frac{\Delta \dot{y}_{\mathrm{m}}}{\Delta x_d} & \frac{\Delta \dot{y}_{\mathrm{m}}}{\Delta z_\gamma} \\ \frac{\Delta \dot{z}_m}{\Delta x_d} & \frac{\Delta \dot{z}_{\mathrm{m}}}{\Delta z_\gamma} \end{bmatrix}^{-1} e_r + \begin{pmatrix} x_{d0} \\ z_{\gamma 0} \end{pmatrix} \tag{43}$$

After applying this method to the initial conditions previously established for the thirty degree chief inclination, the following initial conditions describe the chief's orbit and the relative orbit.

For a given chief orbit:	Desired ROE:
$a = 7000\ \mathrm{km}$	$a_e = 500\ \mathrm{m}$
$\mathrm{e} = 0$	$x_d = 68.35\ \mathrm{cm}$
$\mathrm{i} = 30^\circ$	$y_d = 0\ \mathrm{m}$
$\Omega = 0^\circ$	$\beta = 0^\circ$
$\omega = 0^\circ$	$\gamma = 90.4442^\circ$
$\nu = 0^\circ$	$z_{\max} = 500\ \mathrm{m}$

These initial conditions were propagated for twenty-five orbits and the drift rates in the y and z directions are shown in Figures 17 and 18.

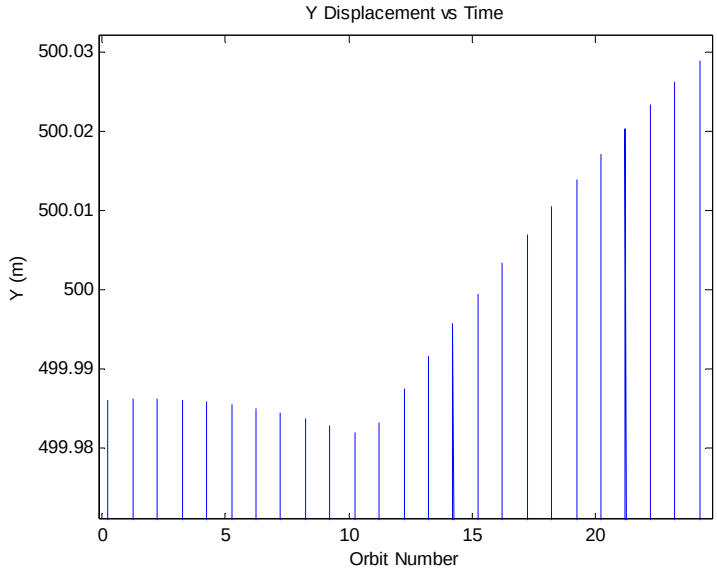

Figure 17: Secular Drift in Y-Direction from Two-Variable Non-Linear Method

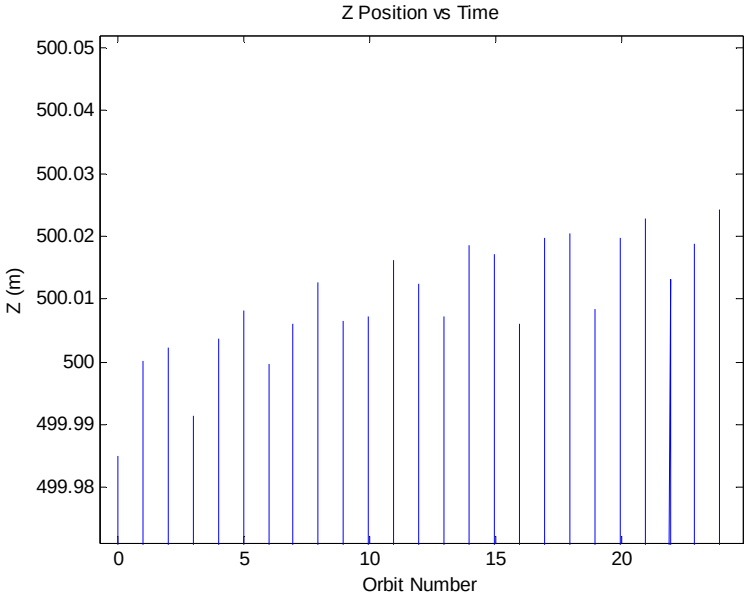

Figure 18: Secular Drift in Z-Direction from Two-Variable Non-Linear Method

Figures 17 shows that the secular drift in the y-direction has been successfully reduced to under 5 cm for the propagation period shown. Figure 18 shows that this method has been able to reduce the secular drift in the z-direction to approximately 3 cm for the propagation period. This is a significant improvement over the approximately 20 cm seen with the single variable method.

V. Results and Discussion

Circular Chief

After verifying that the single-variable non-linear method was now successful, a series of inclinations were used to further analyze this method. Additional inclinations will include the inclination of the international space station, the critical inclination, a true polar orbit, and a sun-synchronous orbit. The initial conditions are

Chief Orbital Elements:

$$a = 7000\,\text{km}$$
$$e = 0$$
$$\Omega = 0^\circ$$
$$\omega = 0^\circ$$
$$\nu = 0^\circ$$

ROE:

$$a_e = 500\text{m}$$
$$y_d = 0\,\text{m}$$
$$z_{\max} = 500\text{m}$$
$$\beta = 0^\circ$$

Chief Inclinations:

$$i = \begin{bmatrix} 30^\circ \\ 51.6^\circ \\ 63.4^\circ \\ 90^\circ \\ 95.4^\circ \end{bmatrix}$$

After applying this method for these chief inclinations the resulting initial conditions were determined and can be seen in Table 1.

Inclination	x_d	γ
30° Inclination	67.2 cm	89.582°
International Space Station (51.6º)	67.7 cm	90.213°
Critical Inclination (63.4 º)	68.1 cm	90.173°
Polar Orbit (90º)	67.8 cm	90°
Sun Synchronous (95.4º)	67.8 cm	90.463°

Table 1: Determined Initial Conditions for Propagated Orbits

After propagating the initial conditions for the given cases the drift in the *z* and *y* directions was plotted in Figures 19 and 20. The magnitudes of the deviation were taken and all cases were plotted together in order to allow for a better visual comparison.

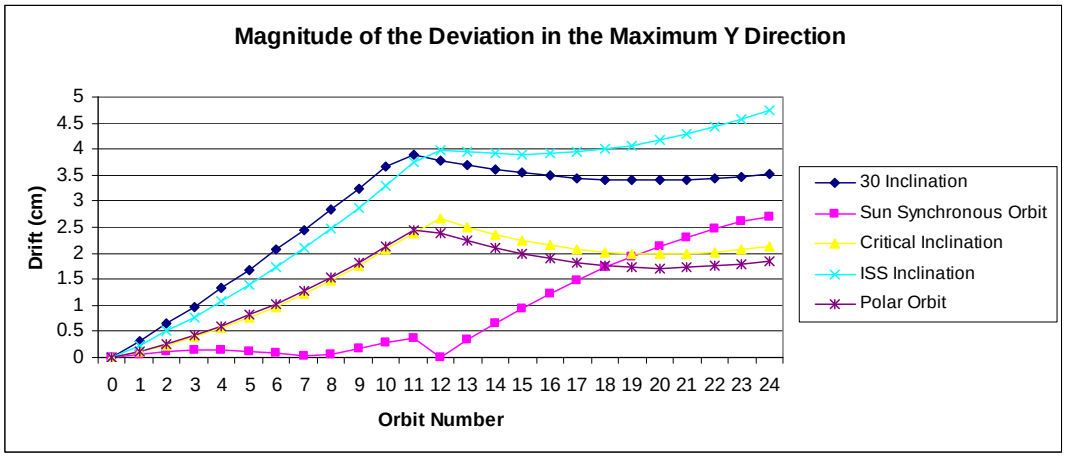

Figure 19: Magnitude of the Deviation in the Maximum Y-Direction

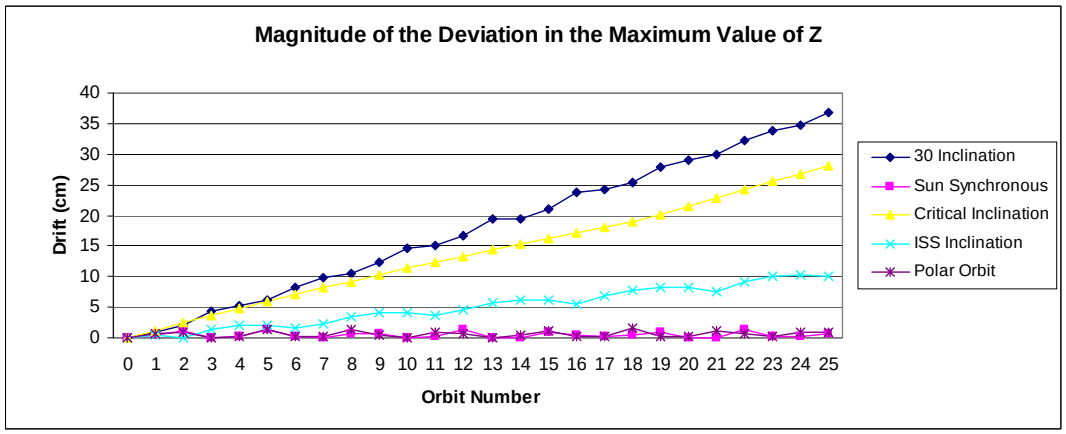

Figure 20: Magnitude of the Deviation in the Maximum Z-Direction

Figure 19 shows that this method is quite successful at canceling out secular drift in the orbital direction, with the worst case producing less than 5 cm drift over the twenty-five orbit propagation period. Also, with approximately three centimeters separating the best from the worst case, this method appears highly consistent across the range of inclinations tested. Figure 20 shows that the ability to minimize the secular drift in the *z*-direction is much less consistent across the inclinations tested. This figure does however show that this method appears highly successful at inclinations at and near 90º. In order to confidently establish the approximate rates of change, these values were put through a linear best fit. The slopes were determined in units of centimeters per orbit and have been listed in Table 2.

Inclination	Drift Rate of z_{max} (cm/orbit)	Drift Rate of y_d (cm/orbit)
30° Inclination	-1.48	-0.13
International Space Station	0.43	-0.19
Critical Inclination	1.08	-8.80E-02
Polar Orbit	-1.02E-02	-7.04E-02
Sun Synchronous	4.11E-03	0.12

Table 2: Drift Rates of Maximum Displacements in Z and Y Directions in cm/orbit

Non-Circular Chief

This method allows for a J_2 invariant solution for two satellites by establishing $\delta(\dot{M}+\dot{\omega})$ and $\delta\dot{\Omega}$ both equal to zero. However, if it is possible to also set $\delta\dot{\omega}$ to zero then it might be possible to lift the circular chief assumption. Fortunately, if both satellites were operating at the critical inclination then this condition would be met. The eccentricity of the chief was chosen such that the difference between the radius at perigee and apogee would be 1000 km. Also, the semi-major axis has been increased to 7500 km to keep a safe altitude while at the radius of perigee. The eccentricities have been chosen to produce a difference in the radii of apogee and perigee of approximately 1000 km and 100 km respectively.

The following initial conditions have been chosen:

Chief Orbital Elements:

$$a = 7500 \text{ km}$$
$$i = 63.4^\circ$$
$$\Omega = 0^\circ$$
$$\omega = 0^\circ$$
$$\nu = 0^\circ$$

Desired ROE:

$$a_e = 500\text{m}$$
$$y_d = 0\,\text{m}$$
$$z_{\max} = 500\text{m}$$
$$\beta = 0^\circ$$

The corresponding calculated values for the initial conditions are shown in Table 3.

	Eccentricity	x_d	γ
Case 1	0.0667	77 cm	90.241°

Case 2	0.00667	60.8 cm	90.190°

Table 3: Initial Conditions for Non-Circular Chief

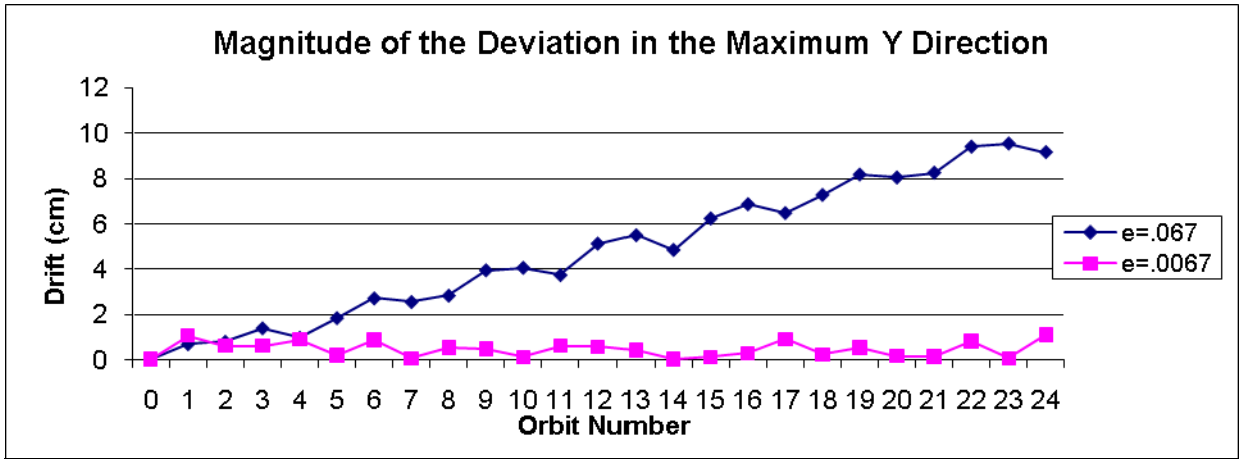

Figure 21: Magnitude of Drift in Y-Direction for Non-Circular Chief Orbits

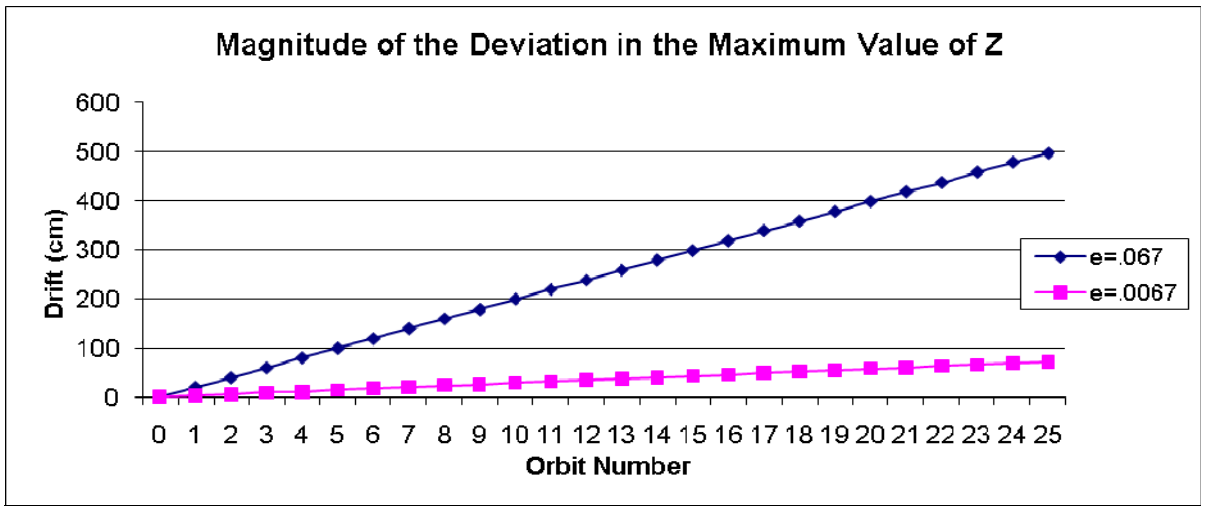

Figure 22: Magnitude of Drift in Z-Direction for Non-Circular Chief Orbits

Figure 21 shows that the case of a moderately eccentric chief is not as successful at canceling the drift in the orbital direction; while the case for small eccentricity chief produced results as accurate as those produced for a circular chief. Unfortunately, Figure 22 shows that this method is nowhere near as successful at eliminating the drift in the *z*-direction for the moderate eccentricity chief orbit.

Although it is difficult to see due to the scale of Figure 22 the drift rate in the *z*-direction is approximately thrice the drift seen for the circular chief with the same inclination. It is true that the difference in semi-major axis is approximately 500 km; however, the case was rerun at a matching semi-major axis and produced similar results. In order to determine if these results were an isolated case, the same eccentricity of .0067 was also simulated at the ISS inclination. The resulting ROE are given in Table 4.

	Eccentricity	**Inclination**	x_d	γ
Case 1	0	63.4°	68.1 cm	90.173°
Case 2	0.0067	63.4°	68.1 cm	90.2128°
Case 3	0	51.6	67.7 cm	90.213°
Case 4	0.0067	51.6	70.0 cm	90.1781°

Table 4: Initial Conditions for Circular and Near Circular Comparisons

The initial conditions were propagated once again for 25 orbits, producing the results shown in Figure 23.

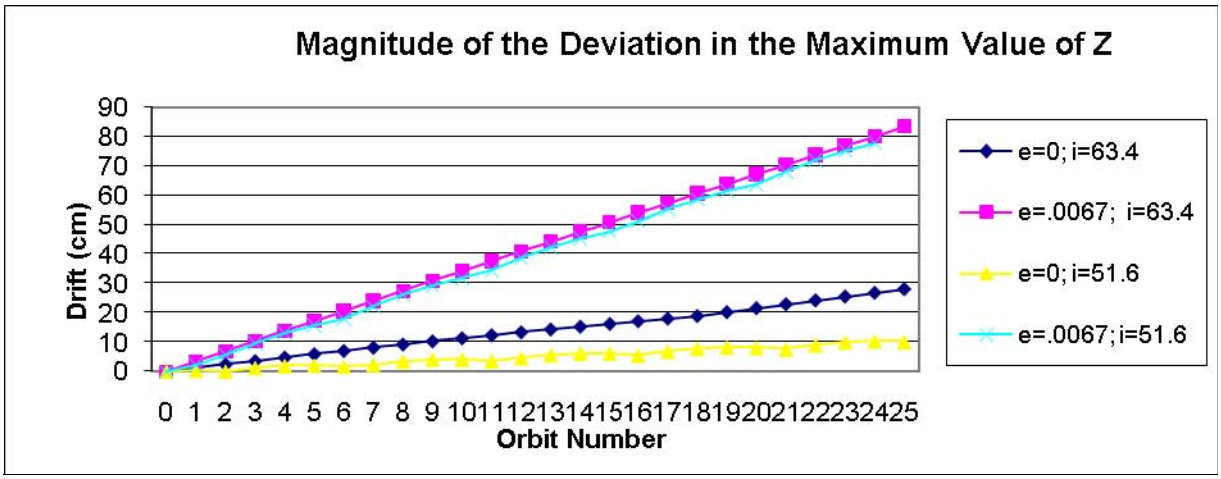

Figure 23: Deviation in the Z-Direction for Circular and Near Circular Chief Orbits

It can be seen from Figure 23 that the method appears to produce larger out-of-plane drift for a near circular chief multiple than it does for a circular chief.

Additional Drift Rates

With the previous case for non-circular chief at ISS inclination, the initial primary concern was the drift secular drift in the argument of perigee. In order to determine the effects due to secular drift of the argument of perigee, the maximum displacement in the *x*-directions were also compared. It turns out that the previous notion of occupying the critical inclination in order to reduce the secular drifts in the difference of the argument of perigee was somewhat effective; however, even when the chief occupied the ISS inclination the secular drift in the *x*-direction was considerably smaller than the drift in the *z*-direction, as seen in Figure 24.

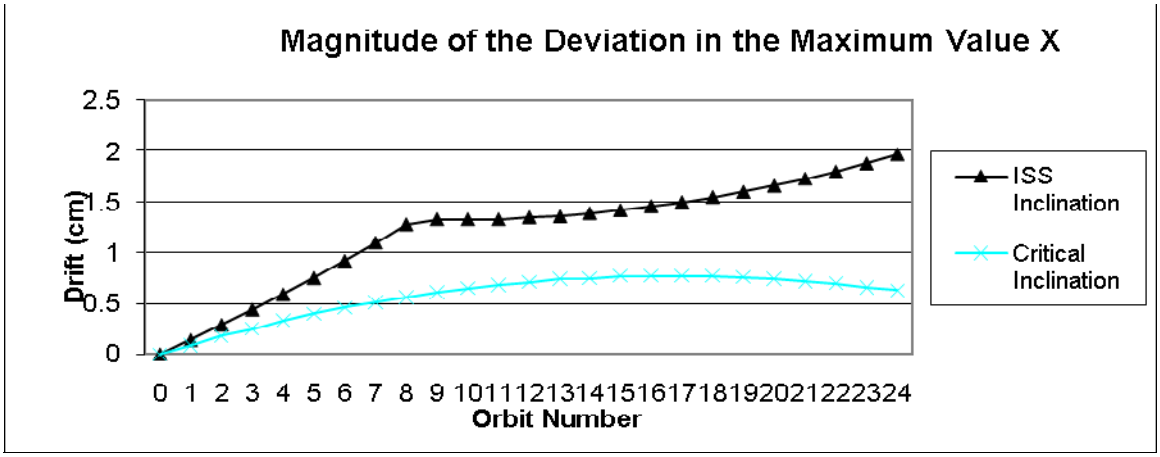

Figure 24: Magnitude of the Deviation in the Maximum Value of X for Non-Circular Chiefs

It turns out that the drift rate produced in the *x*-direction is not only small, but it is actually less than the drift in the *y*-direction. This is partially due to the initial conditions that established the difference in the argument of perigee, $\delta\omega$, to be near zero. Applying this to a small angle approximation would result in the drift in the *x*-direction to be approximately on the order of the $\delta\omega^2$. In an attempt to maximize the drift rate in the *x*-direction the case was run again with the arguments of perigee with a 90° separation. In this case the secular drift for the 25 orbit propagation was approximately 7.5 cm. However, the size of the relative orbit was increase drastically. If taking into consideration that the new a_e had increased to over 100 km, it is easy to see that the percent difference between the secular drift and the relative major axis is considerably small. Unfortunately, with such an increase in the size of the relative orbit, it was also concluded that this method is considerably less flexibility in the initial value of β. Therefore, in order to maintain the flexibility in the ROE the case if a non-circular chief will be deemed impractical and additional work in this thesis will only consider the case of the circular chief reference orbit.

Two-Variable Non-Linear Method

After determining from Figure 20 that the single-variable method was unable to produce accurate results for all inclinations, the two-variable method was used at 30° chief inclination. The results are plotted in Figure 25.

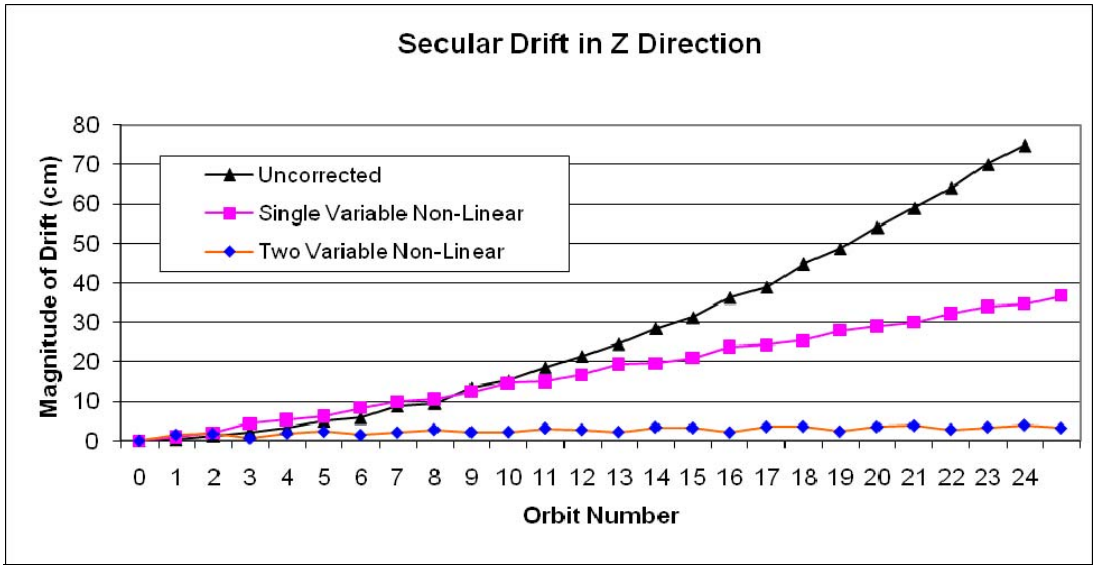

Figure 25: Comparison of Secular Drifts in Z Direction

It is easy to see in Figure 25 that for a chief inclination of 30°, the two-variable non-linear method is much more successful at reducing the secular drift in the *z*-direction than the single-variable method. Therefore, the method will be applied to the other inclinations whose secular drifts from the single-variable method were still large. The following initial conditions will be used with chief orbital inclinations 30°, ISS inclination, and Critical Inclination. The resulting ROE were calculated and are displayed in Table 5.

Chief Orbital Elements:

$$a = 7500 \text{ km}$$
$$e = 0$$
$$\Omega = 0^\circ$$
$$\omega = 0^\circ$$
$$\nu = 0^\circ$$

Desired ROE:

$$a_e = 500\text{m}$$
$$y_d = 0\,\text{m}$$
$$z_{\max} = 500\text{m}$$
$$\beta = 0^\circ$$

Inclination	x_d	γ
30° Inclination	68.35 cm	90.444°
International Space Station (51.6º)	67.86 cm	90.031°
Critical Inclination (63.4 º)	67.87 cm	90.044°

Table 5: Initial Conditions for Two-Variable Non-Linear Method

After propagating these initial conditions the secular drift in the *z*-direction was plotted in Figure 26.

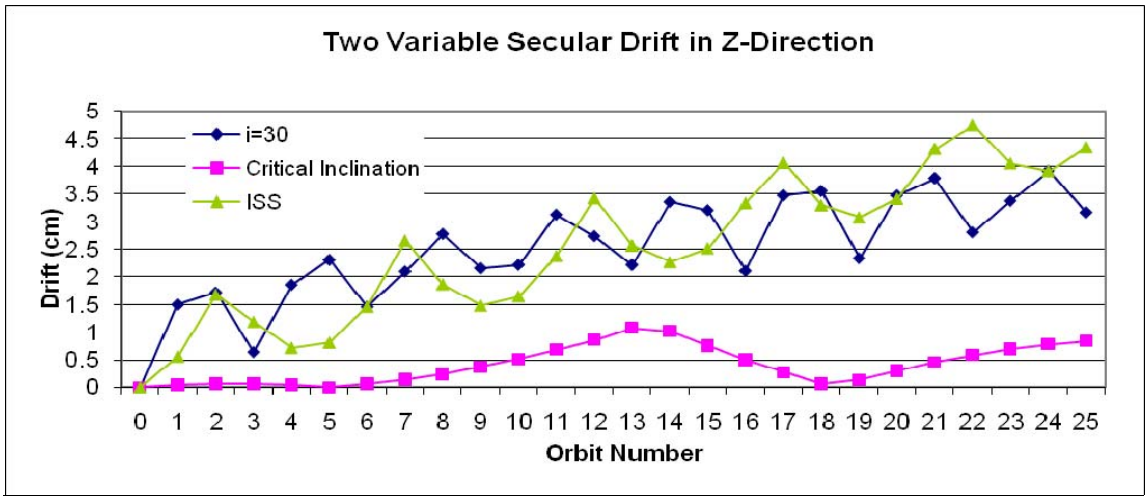

Figure 26: Secular Drift in Z-Direction for Multiple Chief Inclinations

Figure 26 shows that this method is successful at reducing the secular drift in the *z*-direction to fewer than 5 cm over the propagation period of 25 orbits. The secular drift in the *y*-direction is plotted in Figure 27.

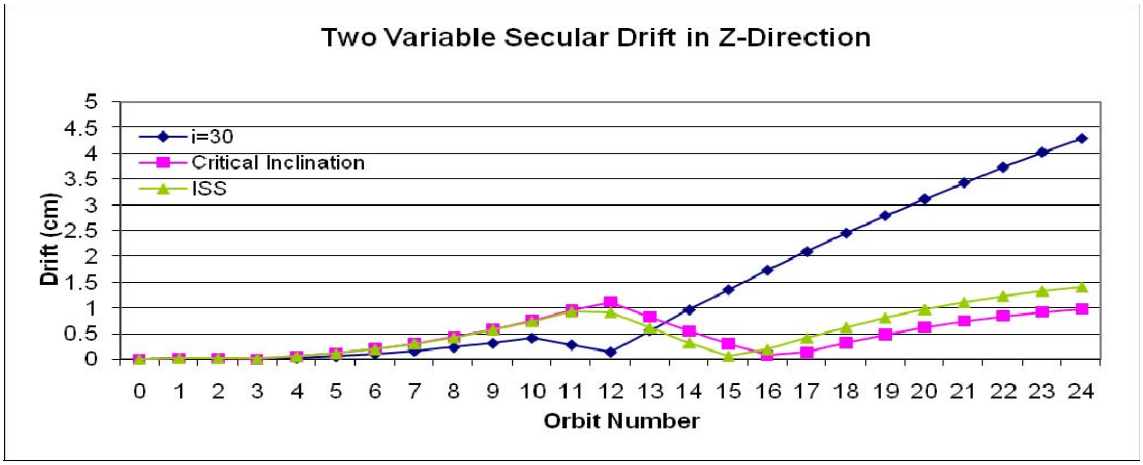

Figure 27: Secular Drift in *Y*-Direction for Multiple Chief Inclinations

It is apparent from Figures 26 and 27 that the method has successfully reduced the secular drifts in both directions to the same order.

After verifying that the method has successfully reduced the secular drift in the *z*-direction the two-variable method's initial conditions for these three inclinations were compared with the single-variable near-polar results.

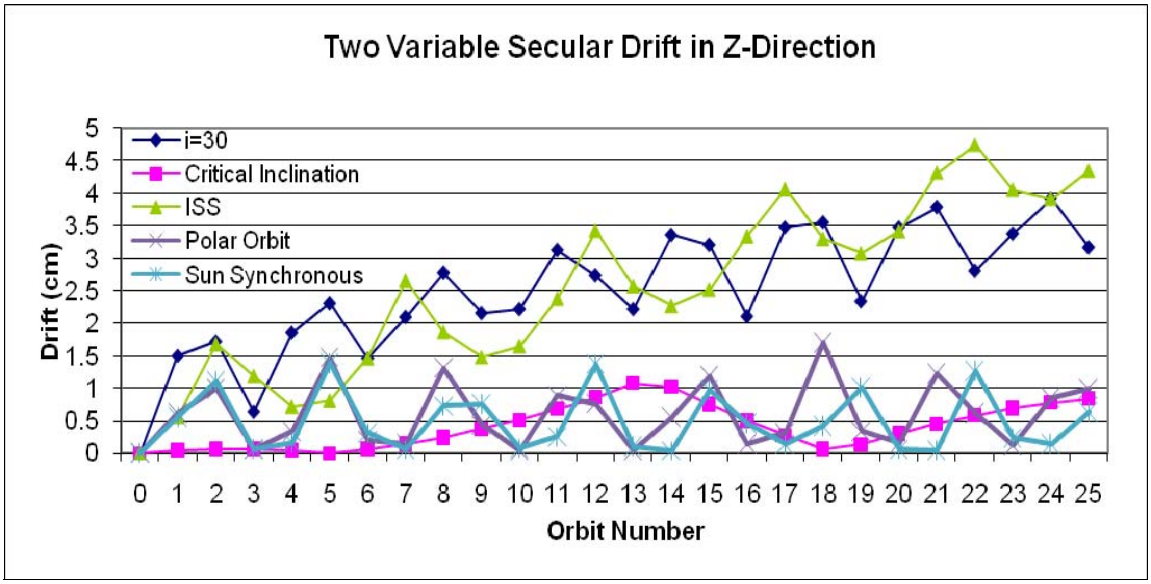

Figure 28: Comparison of Single-Variable and Two-Variable Non-Linear Methods

Figure 25 shows that the two-variable method has produced significantly more accurate results than the single-variable method for a 30° chief inclination. However,

Figure 28 shows that the method is still dependant on the chief's inclination; with the critical-inclination being the only inclination in this set that is able to produce results as accurate as the near-polar results for the single-variable method.

VI. Conclusion

This thesis approached the problem of establishing J_2 invariant formations by setting the chief's COE and stating a desired set of ROE. It was then determined that the two ROE, x_d and γ, could be adjusted in order to reduce the secular effects of this perturbation acceleration. This work consisted of establishing a non-linear method for determining the ROE x_d. Once this method had produced desirable tolerances in the secular drift rate in the orbital direction the value of x_d was used in a linear function to solve for the angle of the oscillation in the z-direction. With this value and an arbitrary selection of the angle β the angle γ was calculated, completing the set of initial conditions.

After establishing a single-variable non-linear method to produce the initial conditions, the process was run with various chief inclinations. The results showed that the method was consistent at producing secular drifts of approximately two to five centimeters drift in the orbital direction over the 25 orbit propagation period. Unfortunately, the secular drift rate in the out-of-plane direction was less consistent across the inclinations, with the worst drift being 1.4 centimeters per orbit at an inclination of 30° and the best being approximate 41 micrometers per orbit at 95°. This suggests that the ability of this method to reduce the secular drift in the z-direction is somewhat dependent on the inclination. According to the paper done by Sabatini (5:97-100) this is also the case with the J_2 invariant method developed by Schaub and Alfriend (6:77-95). However, the previous method showed most desirable results at the critical inclination, whereas this method produces optimum results at near polar orbits.

When the method was extended to include non-circular chief orbits, the method was less successful at producing small drifts in the out-of-plane direction; producing drift rates of over 3 centimeters per orbit. However, it was shown that the method was still able to produce relative stability in the *x*-direction, with less than 2 centimeters drift after propagating the initial conditions for 25 orbits. Unfortunately, when attempting to control the initial relative angle β the size of the relative orbit increased by over 100 km. This is due to the moderately large eccentricity of the chief's orbit and the difference in the argument of perigee required to induce the initial relative angle. This suggests that in order to maintain flexibility of the deputy's position on relative orbit the chief will have to be at a near zero eccentricity.

After determining that the single-variable method was unable to produce desirable drift rates for all inclinations, the single-variable method was then extended to solve for both variables simultaneously. This two-variable non-linear method produced significantly more accurate results for the lower inclinations; however, even with increased accuracy in the lower inclinations, the method was not always able to reproduce the accuracy established by the single-variable method for near polar orbits. This suggests that if it is possible to place a formation at inclinations around or above the critical inclination, one of these two methods will be able to establish near J_2 invariance. Fortunately, even if this is not possible, these results do show that the two-variable non-linear method will be able to significantly reduce the secular drifts due to the perturbing accelerations.

Future Work

Further work on this subject could include considering the stability of multiple satellite formations. By declaring certain deputies as "sub-chiefs" it would be possible to

determine the ROE between the sub-chiefs and the deputies. This could be repeated until the relative geometry between all of the satellites in the formation has been determined. This would allow for a better understanding of more advanced formations; where the relative geometries between the chief and deputies are a concern, as well as the relative geometries between deputies. This information could also simplify the task of deconflicting the trajectories of multiple deputies, and decreasing the possibility of a collision. Additional work could attempt to further refine the relative positions in an attempt to achieve specific geometric shapes at a desired argument of latitude. This could aid in spreading the system out normal to a point of interest, and allow for a broader distributed aperture system.

Bibliography

1. Breger, L., How, J., and Alfriend, K. T., "Partial J_2 Invariance for Spacecraft Formations," Paper No. AIAA 2006-6585, AIAA/AAS Astrodynamics Conference, Keystone, CO, Aug. 2006

2. Gim, D. W., and Alfriend, K. T., "State Transition Matrix of Relative Motion for the Perturbed Noncircular Reference Orbit," *Journal of Guidance, Control, and Dynamics*, Vol. 26, No. 6, 2003, pp. 956–971.

3. Lovell, T. A., and Tragesser, S. G., "Guidance for Relative Motion of Low Earth Orbit Spacecraft Based on Relative Orbit Elements," AIAA/AAS Astrodynamics Specialist Conference and Exhibit, Province, RI, AIAA Paper 2004-4988, 2004

4. Luck, James and Lovell, T. Allen, "Linear Mapping Between Hill Frame Coordinates and Orbital Element Differences," Unpublished Paper, Air Force Research Lab: Space Vehicles Directorate, 2007

5. Sabatini, M, Izzo, D., and Bevilacqua, R., "Special Inclinations Allowing Minimal Drift Orbits for Formation Flying Satellites," *Journal of Guidance, Control, and Dynamics*, Vol. 31, No. 1, January–February 2008, pp 94-100

6. Schaub, H. and Alfriend, K. T., "J_2 Invariant Relative Orbits for Spacecraft Formations," Flight Mechanics Symposium, (Goddard Space Flight Center, Greenbelt, Maryland), January 18-20, 2002, Paper No. 11, pp. 77-95

7. Schaub, Hanspeter and Junkins, John L. "Analytical Mechanics of Space Systems" American Institute of Aeronautics and Astronautics, Reston, VA, 2003

8. Tragesser, Steven G, and Skrehart, Brent, "Stationkeeping Analysis for Satellite Formations Including Oblateness Perturbations," *AIAA Guidance, Navigation and Control*, Breckenridge, CO Feb. 2007

9. Wie, Bong, "Space Vehicle Dynamics and Control." American Institute of Aeronautics and Astronautics, Reston, VA, 1998

10. Wiesel, William E., "Optimal Impulsive Control of Relative Satellite Motion," *Journal of Guidance, Control, and Dynamics,* Vol. 26, No. 1, 2003, pp. 74-78.

Appendix A: State Transition Matrix

$$A=\begin{bmatrix} \frac{r}{a} & r\frac{V_r}{V_t} & 0 & -\frac{r}{p}(2aq_1+r\cos\theta) & -\frac{r}{p}(2aq_2+r\sin\theta) & 0 \\ 0 & r & 0 & 0 & 0 & r\cos i \\ 0 & 0 & r\sin\theta & 0 & 0 & -r\cos\theta\sin i \\ -\frac{V_r}{2a} & \left(\frac{1}{r}-\frac{1}{p}\right)h & 0 & \frac{V_r aq_1+h\sin\theta}{p} & \frac{V_r aq_2-h\cos\theta}{p} & 0 \\ -\frac{3V_t}{2a} & -V_r & 0 & \frac{3V_t aq_1+2h\cos\theta}{p} & \frac{3V_t aq_2+2h\sin\theta}{p} & V_r\cos i \\ 0 & 0 & V_t\cos\theta+V_r\sin\theta & 0 & 0 & \sin i(V_t\sin\theta-V_r\cos\theta) \end{bmatrix}$$

Where:

$$V_r = \frac{h}{p}(q_1\sin\theta - q_2\cos\theta)$$

$$V_t = \frac{h}{p}(1+q_1\cos\theta - q_2\sin\theta)$$

$$p = a(1-e^2)$$

$$h = |r\times v|$$

Appendix B: Figure of Relative Orbital Elements

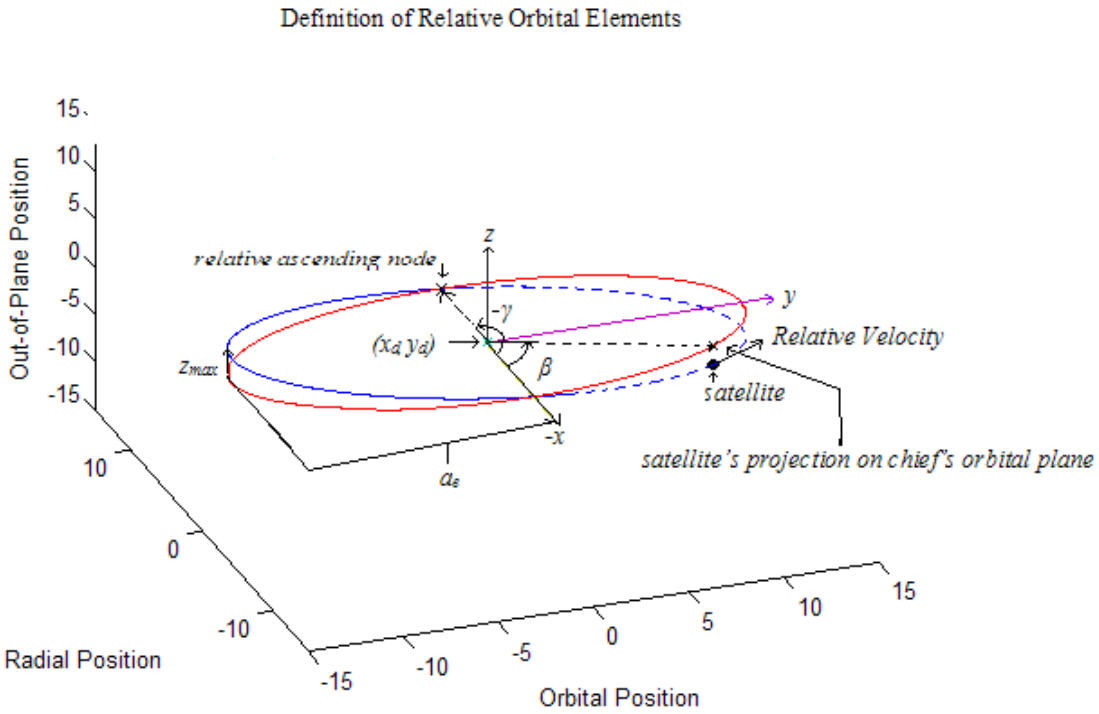

Figure 29: Figure of Relative Orbital Elements

REPORT DOCUMENTATION PAGE		Form Approved OMB No. 0704–0188

1. REPORT DATE (DD–MM–YYYY)	2. REPORT TYPE	3. DATES COVERED (From — To)
14–03–2008	Master's Thesis	Aug 2007 — Mar 2008

4. TITLE AND SUBTITLE	5a. CONTRACT NUMBER
Minimizing Secular J_2 Perturbation Effects on Satellite Formations	5b. GRANT NUMBER
	5c. PROGRAM ELEMENT NUMBER
6. AUTHOR(S)	5d. PROJECT NUMBER
Jonathan W. Wright, 2 Lt, USAF	5e. TASK NUMBER
	5f. WORK UNIT NUMBER

7. PERFORMING ORGANIZATION NAME(S) AND ADDRESS(ES)	8. PERFORMING ORGANIZATION REPORT NUMBER
Air Force Institute of Technology Graduate School of Engineering and Management (AFIT/EN) 2950 Hobson Way WPAFB OH 45433-7765	AFIT/GA/ENY/08-M08
9. SPONSORING / MONITORING AGENCY NAME(S) AND ADDRESS(ES) Dr T. Alan Lovell Space Vehicles Directorate, Air Force Research Laboratory 3550 Aberdeen Ave SE Kirtland AFB, NM 87117	10. SPONSOR/MONITOR'S ACRONYM(S) AFRL/RVES 11. SPONSOR/MONITOR'S REPORT NUMBER(S)

12. DISTRIBUTION / AVAILABILITY STATEMENT

APPROVED FOR PUBLIC RELEASE; DISTRIBUTION UNLIMITED

13. SUPPLEMENTARY NOTES

14. ABSTRACT

The purpose of this thesis is to examine the secular effects of the J_2 oblateness perturbation on close proximity satellites. The main objective is to analyze the deputy's position and velocity with respect to the chief and adjust the initial conditions of the deputy in an attempt to minimize the secular effects of J_2 perturbations. Previous work has provided a method of obtaining a closed form solution for J_2 invariance with co-planar orbits. Therefore, this work will primarily consider deputy orbits that experience motion outside of the chief's orbital plane.
Upon determining the required initial conditions, the invariance will be verified through numerical integration. The method will be considered successful when it is able to reduce secular effects to near numerical tolerances.

15. SUBJECT TERMS

J2 Invariance, ROE, Relative Orbit Elements, Satellite Formations, oblateness perturbation, J2 perturbation, secular effects

16. SECURITY CLASSIFICATION OF:			17. LIMITATION OF ABSTRACT	18. NUMBER OF PAGES	19a. NAME OF RESPONSIBLE PERSON
a. REPORT	b. ABSTRACT	c. THIS PAGE			Nathan A. Titus, Lt Col, USAF
U	U	U	UU	69	19b. TELEPHONE NUMBER (Include Area Code) (937) 255-6565, ext 4597 (Nathan.Titus@afit.edu)